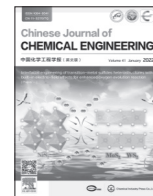




Contents lists available at ScienceDirect

## Chinese Journal of Chemical Engineering

journal homepage: [www.elsevier.com/locate/CJChE](http://www.elsevier.com/locate/CJChE)

## Review

## Reaction kinetics determination based on microfluidic technology

Zifei Yan, Jiabin Tian, Chencan Du, Jian Deng, Guangsheng Luo\*

The State Key Lab of Chemical Engineering, Department of Chemical Engineering, Tsinghua University, Beijing 100084, China



## ARTICLE INFO

## Article history:

Received 21 June 2021  
 Received in revised form 30 August 2021  
 Accepted 30 August 2021  
 Available online 22 October 2021

## Keywords:

Microfluidics  
 Microreactor  
 Kinetics  
 Chemical reaction

## ABSTRACT

Microfluidic technology has been successfully applied to determine the reaction kinetics relying on its great characteristics including narrow residence time distribution, fast mixing, high mass and heat transfer rates and very low consumption of materials. In this review, the recent progresses about the reaction kinetics measured in microreactors are comprehensively organized, and the kinetic modeling thoughts, determination methods and essential kinetic regularities contained in these studies are summarized according to the reaction types involving nitration, oxidation, hydrogenation, photochemical reaction, polymerization and other reactions. Besides, the significant advances in the innovation of micro-platform are also covered. The novel reactor configuration methods were established mainly to achieve rapid and efficient data collection and analysis. Finally, the advantages of microfluidic technology for the kinetic measurement are summarized, and a perspective for the future development is provided.

© 2021 The Chemical Industry and Engineering Society of China, and Chemical Industry Press Co., Ltd. All rights reserved.

## 1. Introduction

Kinetics and thermodynamics are two most important characteristics of a chemical reaction. Thermodynamics determines the necessary conditions for a reaction to occur, as well as its direction and limitation. Kinetics determines the rate of a reaction, closely related to the dimension of time. The kinetic study is essential both in the field of chemistry and chemical engineering. The kinetic study can provide clues to reaction mechanism, helping chemists to grasp the information of the transition state and further understand the pathways of a reaction at the molecular level [1]. In this way, chemists can better design and realize a reaction. For chemical engineers, the kinetic study is the key to know the rate-determining step, and this important information can help them to find the right direction to intensify a reaction and make it more efficient and safer [2]. Furthermore, kinetic data is the foundation to design reactors both in laboratory research and industrial production.

To obtain the kinetics of a reaction, it is necessary to know the relation of the reaction rate with the concentrations, temperature and pressure (Eq. (1)). The establishment of function  $f(C_A, C_B, C_C, \dots, T, P)$  must be based on a deep understanding of the reaction mechanism and the law of interaction between molecules. Every reaction is accomplished *via* a series of elementary

reactions, which follow the law of mass action. Based on the theory of rate-determining step, the overall rate equation can be deduced *via* equilibrium hypothesis [3] or steady-state hypothesis [4]. Sometimes, the function can be expressed as the form of power-law, just like the one shown in Eq. (2). As for the more sophisticated reactions with various interaction steps, the form of the function can become very complex. Eq. (3) shows the kinetic equation of the hydrogenation reaction of carbon monoxide on the Fe–Co–Mn catalyst. The reaction rate constant ( $k$  in Eq. (2),  $k_p$  in Eq. (3)) is strongly affected by temperature, which can be described by Arrhenius formula (Eq. (4)).

$$r = \frac{dC_A}{dt} = f(C_A, C_B, C_C, \dots, T, P) \quad (1)$$

$$f(C_A, C_B, C_C, \dots, T, P) = kC_A^\alpha C_B^\beta C_C^\gamma \dots \quad (2)$$

$$-r_{CO} = \frac{k_p b_{CO} b_{H_2} P_{CO} P_{H_2}}{(1 + 2(b_{CO} P_{CO})^{0.5} + b_{H_2} P_{H_2})^3} \quad (3)$$

$$k = A \exp(-E_a/RT) \quad (4)$$

The accurate measurements of temperature and concentration field, as well as the reaction time are keys to determining reaction kinetics. Moreover, every reaction is definitely tight coupled with mass and heat transfer. Under unfavorable mass transfer condition, the reaction can be controlled by external or internal mass transfer, thus the obtained rate equation can only reflect the characteristics

\* Corresponding author. Fax: +86 62 783 870.  
 E-mail address: [gsluo@tsinghua.edu.cn](mailto:gsluo@tsinghua.edu.cn) (G. Luo).

of mass transfer rather than the chemical reaction itself [5]. Under unfavorable heat transfer condition, the thermal effect of the reaction can influence the temperature distribution, generating local hot or cold spots and thereby seriously interfering with the kinetics determination.

The conventional kinetic measurement is carried out in a stirring tank. The methods of data collecting and processing include: (1) determining the initial reaction rate to fit the kinetic differential equation; (2) determining the change of concentration with reaction time to fit the kinetic integral equation. For some conventional reactions with moderate reaction rate, viscosity, temperature and pressure, the stirring method hold advantages because of its ease of device configuration [6]. However, it has great limitations in some special reaction systems such as fast and highly exothermic reactions, heterogeneous reactions, photocatalytic reactions and so on.

Microfluidic technology has been applied to various research fields including biology, medicine, materials, energy and electronics [7,8], and its application value in kinetic measurement has gradually attracted researchers' attention. As mentioned above, the accurate measurement of temperature and concentration field, as well as their variations with reaction time are the basis of kinetic measurement, and the characteristics of microreactors could perfectly meet these requirements.

The uniform temperature field can be easily acquired because of the fast heat transfer in microreactors. The heat transfer coefficient could reach  $10 \text{ kW} \cdot \text{m}^{-2} \cdot \text{K}^{-1}$ , which is one order of magnitude higher than the conventional heat exchangers [9].

The flow state in microreactors is mostly laminar flow because of the small feature size of 10–500  $\mu\text{m}$ , and by increasing the flow velocity, the plug flow state can be achieved [10]. The dimensionless parameter, Péclet number ( $Pe = uL/D$ ), is often used as a criterion. For many reaction processes in microreactors,  $Pe$  could be larger than 100, indicating that the flow model in the microreactor had a small deviation from the plug flow and thus the backmixing could be ignored. Therefore, the residence time distribution (RTD) can be very narrow. At the same time, the residence time can be designed at the level of sub-second or even sub-millisecond, which determines that microreactors can be used as a strong tool to measure kinetics and regulate reactions in this time scale [11].

The excellent mass transfer performance allows microreactors to be used for intrinsic kinetic measurement by eliminating mixing effect and mass transfer resistance. The enhancement of mixing in microreactors is achieved mainly by shortening the diffusion distance, which is very important especially for the fast reactions like nitration, oxidation and so on [12]. Studies [13] have shown that the mass transfer coefficient in microreactors can achieve  $10^{-4}$  to  $10^{-3} \text{ m} \cdot \text{s}^{-1}$ , which is one order of magnitude higher than that of conventional equipment. Besides, the specific surface area in microreactors can achieve  $10^3$  to  $10^4 \text{ m}^2 \cdot \text{m}^{-3}$ , which is one to two orders of magnitude higher than that of conventional equipment. On the whole, the volumetric mass transfer coefficient in microreactors is 10–1000 times higher than that of conventional equipment. The dimensionless parameter, Hatta number ( $Ha$ ), which represents the relative speed of the reaction rate to the mass transfer rate, is often calculated to be lower than 0.3 [14]. Therefore, the effect of external mass transfer resistance can be easily eliminated in microreactors [15].

When using solid catalyst, the internal mass transfer can exert great influence on kinetics. In microreactors, this effect can be inhibited by reducing the thickness of catalyst layers [16] or by reducing the catalyst particle size in the slurry-flow microreactors [17]. The dimensionless number, Thiele modulus ( $\phi$ ), is often used to describe the effect of internal mass transfer. And some studies indicated that, in microreactors,  $\phi < 6 \times 10^{-4}$  can be realized for

heterogeneously catalytic reactions [18], which means that the internal mass transfer could be ignored.

Another advantage of microreactor is its small volume and very little reagent consumption. This characteristic provides convenience for the studies on the reactions whose reagents or catalysts are hard to obtain or prepare [1], and also provides safe guarantee for kinetic measurement. Besides, the unidirectional flow characteristic in microreactors is conducive to the combination of inline analysis and feedback control to automate the experiments, which can significantly improve the data collection and testing efficiency [19].

The objective of this review is to present the state of the art of kinetic studies in microreactors. Flow, mixing, mass and heat transfer characteristics in microdevices are not the focuses of this work, the relevant content can be referred to the previous review articles [13,20–23]. In section two, the configuration of microdevices is the focus, including the discussion about kinetic modeling, micro-platform construction and testing methods, all of which are developed to realize accurate, rapid and flexible kinetic measurement. In section three, the reaction kinetics of nitration, oxidation, hydrogenation, photochemical reaction, polymerization is discussed respectively, evaluating the key role played by microreactors in combination with the specific reaction types. Finally, a perspective for the development of microfluidic technology in kinetic measurement is provided in section four.

## 2. Micro-Platform Innovation for Kinetic Measurement

### 2.1. Inline analysis method

The residence time in microreactors is basically measured according to the reactor volume and flow rate. In order to acquire the precise residence time for kinetic measurement, the reaction must be inline quenched and preserved for off-line analysis. The inline analysis methods can significantly improve the testing efficiency. Up to now, UV/visible spectrophotometry [24–26], Fourier transform infrared spectroscopy [11,27], HPLC [19] and GC [28] have been in-situ combined with microfluidic technology for kinetic measurement.

Benito-Lopez *et al.* [24] developed a quartz capillary microreactor combining the inline UV/Vis spectrophotometry to obtain the kinetics of the nucleophilic aromatic substitution and Diels–Alder reactions under high pressure condition. The process safety was effectively improved by using a miniaturized (3 ml volume) reaction system. As shown in Eq. (5), similar to the concept of activation energy and its definition in Arrhenius equation, the parameter, activation volume ( $\Delta V^\ddagger$ ) was determined to describe the effect of pressure on the reaction rate. Muto *et al.* [25] established a coaxial microporous mixer (pore diameter = 0.05 mm) in combination with a capillary microreactor embedded with a static mixer to measure the kinetics of acetone iodation reaction based on inline analysis of  $\text{I}_3^-$  by UV/Vis spectrophotometry. The obtained activation energy was  $91 \text{ kJ} \cdot \text{mol}^{-1}$ , agreeing well with the value in literatures.

$$\left(\frac{\partial \ln k}{\partial p}\right)_T = -\Delta V^\ddagger / RT \quad (5)$$

Compared with UV/Vis, HPLC can provide more detailed information and has wider applicability because it can separate each substance in the testing solution. McMullen and Jensen [19] constructed a micro-platform for rapid determination of Diels–Alder reaction kinetics with inline HPLC. Except for inline data collection, they further developed inline data analysis (Fig. 1). By establishing a negative feedback adjustment network, the computer can automatically control the reaction temperature, residence time and material concentration to obtain the kinetic data within a mini-

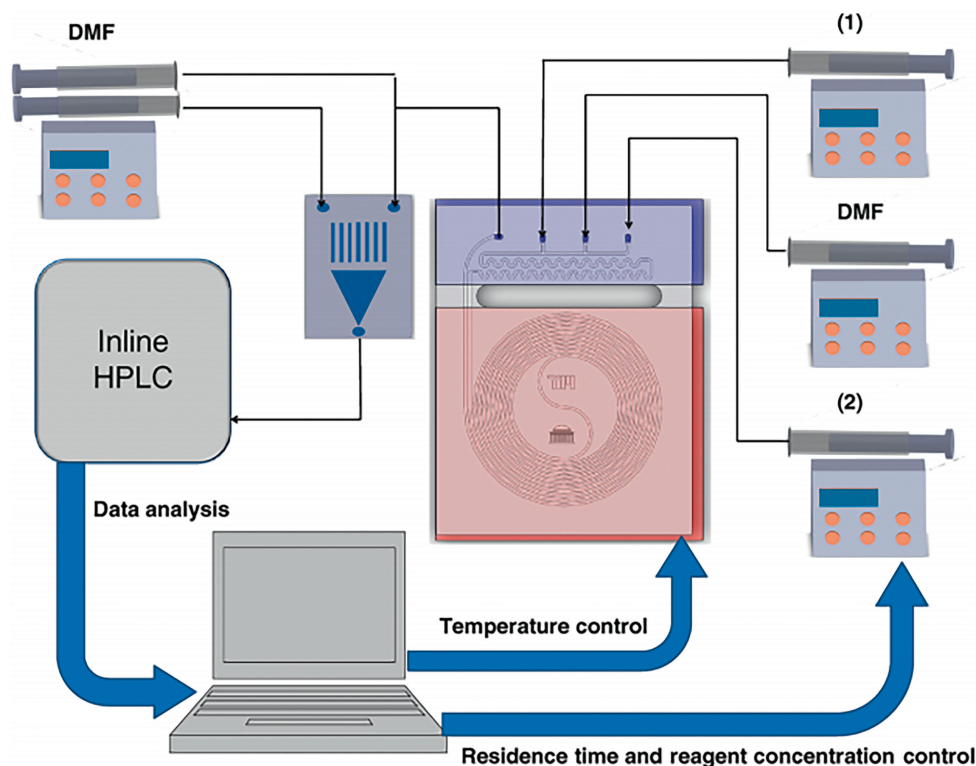


**Fig. 1.** Inline data collection by HPLC and the concept of negative feedback network for kinetic measurement of Diels-Alder reaction. Adapted with permission of American Chemical Society.

imum number of experiments. The obtained kinetic model was validated by scaling the reaction by a factor of 500 in a commercial microreactor system.

Determination of extremely fast reactions (sub-second reactions) has higher requirements for inline analysis because the dead time introduced by detecting instrument can exert great effect on the reaction time. A microreactor coupled with laser based mid-IR chemical imaging was reported by Keles *et al.* [11], and the sub-second organometallic addition reaction of lithium diisopropylamide with phenyl isocyanate was studied in it. As shown in Fig. 2, through the in-situ visual detection of the infrared spectrum whose intensity varied continuously with the channel position, the change of substance concentrations over residence time can be obtained directly from image recognition. However, the current equipment can only measure reaction kinetics at room temperature. The temperature control system should be further developed for measurement in wider temperature ranges.

## 2.2. Multiple results in a single test

The batch operation is under non-steady state condition, which provides convenience for kinetic measurement. The original kinetic results of the change of substance concentration over reaction time can be obtained from a single experiment by continuously taking samples from the batch reactor. However, the operation mode of kinetic measurement in microreactors is based on steady state. Sampling process is performed only when the flow system reaches steady [26]. As a result, the kinetic measurement in continuous flow mode needs more sets of experiments, which will significantly reduce testing efficiency and increase reagent consumption.

In order to acquire multiple kinetic results in a single test, the non-steady state operation mode is introduced in microfluidic technology. With the continuous development of the material con-

veying system and temperature control system, the flow rate and temperature can continuously vary with time according to the pre-set program [27,29]. Duan *et al.* [26] utilized the linear decrease of liquid flow rate, which is called the flow rate ramping method, to determine the kinetics of hydrogenation of nitrobenzene and  $\alpha$ -methyl styrene (see Fig. 3). The residence time continuously increased as the liquid flow rate declined (Fig. 3(b)), the inline UV/Vis spectrophotometry recorded these continuous changing signals to determine the reactant conversion at different residence times (Fig. 3(c) and (d)).

The continuously changing of temperature can also be conducted to measure the activation energy in one set of experiment. Moore *et al.* [27] combined the transient temperature ramping method and inline IR analysis to study the selectivity and kinetics of carbonylation of aryl bromides. It was proved that the rate-determining step was different at different temperature ranges, thereby exhibiting totally different selectivity. The conditions of temperature ramping method are more stringent than flow rate ramping method because the temperature itself affects the reaction kinetics. Taking a fluid particle as the research object, within the range of residence time (for a fluid particle to flow into and flow out the reaction system), the change in temperature must be ignored and the reaction should be considered to perform in a uniform temperature field. Thus, the rate of temperature ramping must be designed to match the residence time.

Temperature is a more easily detected quantity compared with concentration. For reactions with strong thermal effects, temperature changes can reflect the progress of a reaction. Specifically, if an exothermic reaction is carried out in an ideal adiabatic system, the heat released by the reaction can be completely absorbed by the solution. In this way, the total exothermic heat can be obtained according to the temperature rise and the heat capacity of the reaction system, and then the conversion rate can be calculated by

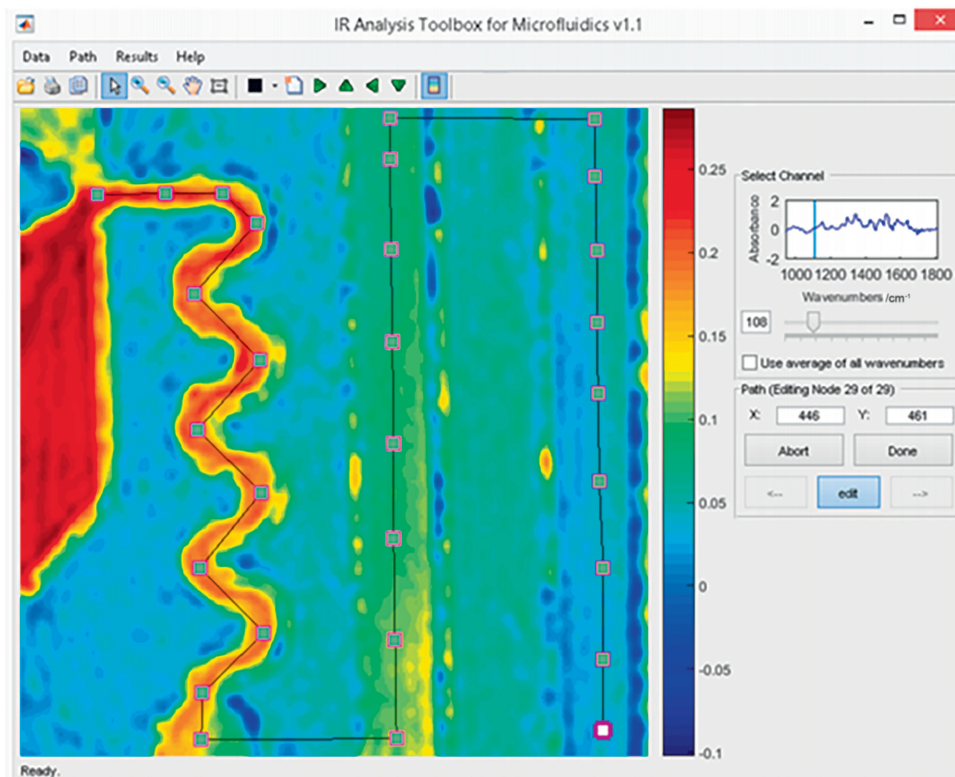


Fig. 2. Infrared spectrum scanning of reaction solution continuously changing with the channel position. Adapted with permission of American Chemical Society.

dividing the total heat by molar reaction heat. Measuring kinetics by adiabatic temperature rise is based on this principle. Moreover, multiple sets of kinetic data can be acquired from a single adiabatic reaction experiment by continuously measuring the temperature change along the microreactor tube. Wang *et al.* [30] developed an adiabatic micro-platform to study the fast-exothermic reaction between cyclohexanecarboxylic acid and oleum. The temperature detection was realized by installing eight sensors along the metal capillary (see Fig. 4).

Infrared thermography is a non-invasive temperature detection method, which doesn't change the flow dynamics inside the microreactor [31]. As shown in Fig. 5(a), a vacuum-adiabatic microsystem was established by Zhang *et al.* [32]. An infrared camera was installed on the top of the vacuum box to receive the infrared signal from the coiled capillary through a window made of  $\text{CaF}_2$  or  $\text{BaF}_2$ , which provides a relatively high and constant transmissivity to the infrared ray. In this way, the total temperature field can be obtained with very high resolution (Fig. 5(b)). The concept of this platform was applied for kinetic measurement of hydrolysis of ethyl acetate [31] and diazotization of ethyl glycinate hydrochloride [9]. Considering the effect of temperature on reaction kinetics, the data processing method to fit kinetic parameters under adiabatic condition is different from the typical one under constant temperature conditions [33]. However, if the temperature rise is too small to affect the reaction rate, the pseudo-constant temperature model is also applicable [31].

Some interesting methods have been developed to further improve the testing efficiency and minimize the reagent consumption in kinetic measurement based on microfluidic technology. Grant *et al.* [34] constructed a microfluidic device that incorporates a functionalized self-assembled monolayer to inline record the "footprint" of a chemical reaction. When the reaction solution flow through the microchannel, the reaction and product molecules could interact with the substrate, thereby leaving recognizable

chemical signals (see Fig. 6). These signals contained the information of substance concentrations can be used to resolve kinetics by laser desorption/ionization mass spectrometry. Fradet *et al.* [35] developed a single-droplet microreactor and a reaction-diffusion (R-D) mathematical model to characterize the reaction kinetics based on the fusion process of reactant droplets. Only 20 nl volume of reagent was consumed in each measurement.

When one reactant is in gas phase, the stable monodisperse bubble-flow pattern can be realized in microreactors. Combined with online microscopic imaging system, the reaction rate can be measured according to the decrease rate for bubble volume. Based on this principle, Zheng *et al.* [36] studied the absorption kinetics of carbon dioxide in 2-amine-2-methyl-1-propanol solution, and proved that the overall adsorption rate in aqueous solution was much higher than that in non-aqueous solution.

### 3. Kinetic Measurement of Different Reaction Systems in Microreactors

In this section, the reaction systems are divided into six categories, namely (1) nitration, (2) oxidation, (3) hydrogenation, (4) photochemical reaction, (5) polymerization and (6) other reactions. In different categories, the microfluidic technology plays different roles in kinetic measurement. However, the basic principle remains the same, which is to make the process safer and more efficient, and make the results more accurate and reliable.

#### 3.1. Nitration

The mixed acid (nitric acid and sulfuric acid) is the most commonly used nitrating agent, almost one-third of reports used mixed acid for aromatic nitration over the last 50 years [37]. Sulfuric acid functions as the dehydrant and catalyst, provides hydrogen

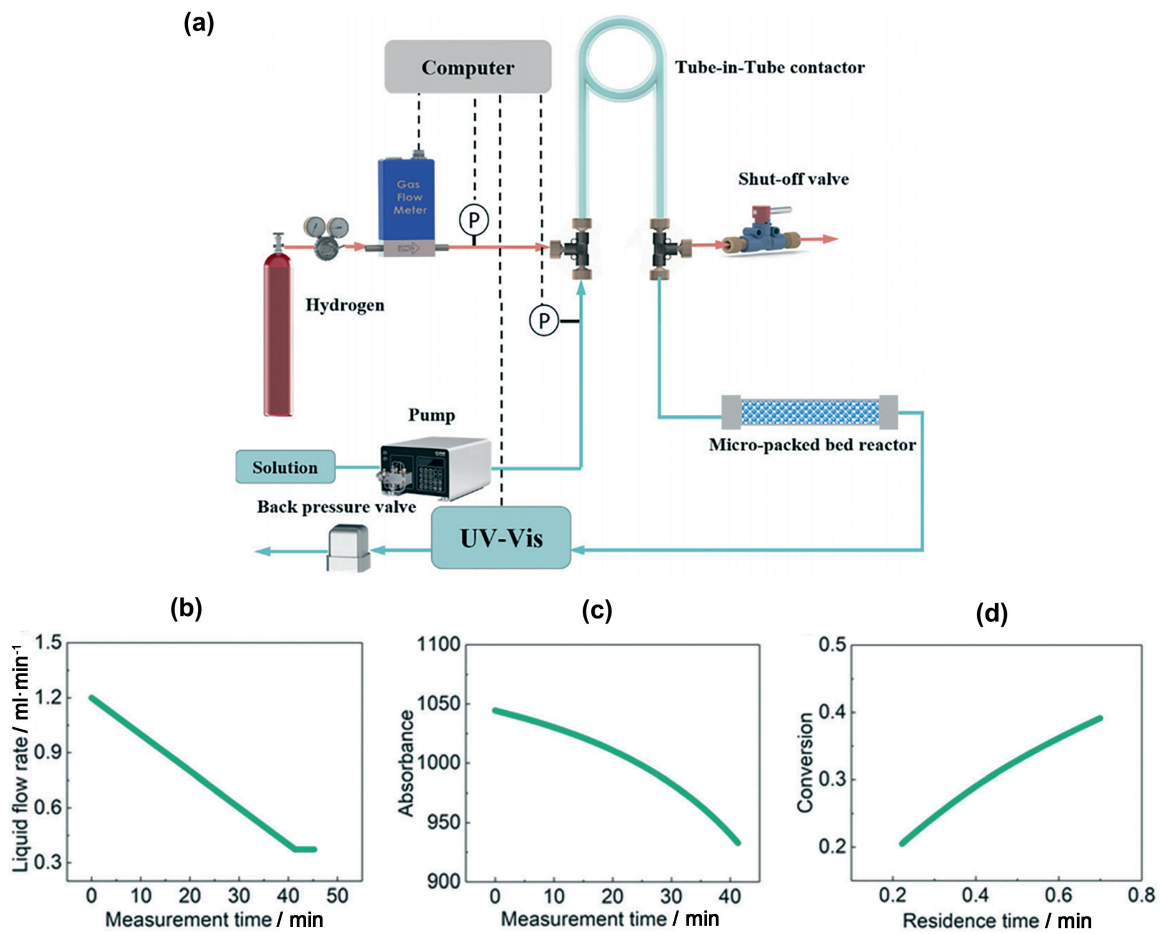


Fig. 3. (a) Schematic of the automated flow system for the accurate determination of gas-liquid-solid hydrogenation kinetics. (b) Flow rate ramping from 1.2 ml·min<sup>-1</sup> to 0.37 ml·min<sup>-1</sup>. (c) Absorbance of  $\alpha$ -methyl styrene at various measurement times. (d) Conversion of  $\alpha$ -methyl styrene at various residence times. Adapted with permission of Royal Society of Chemistry.

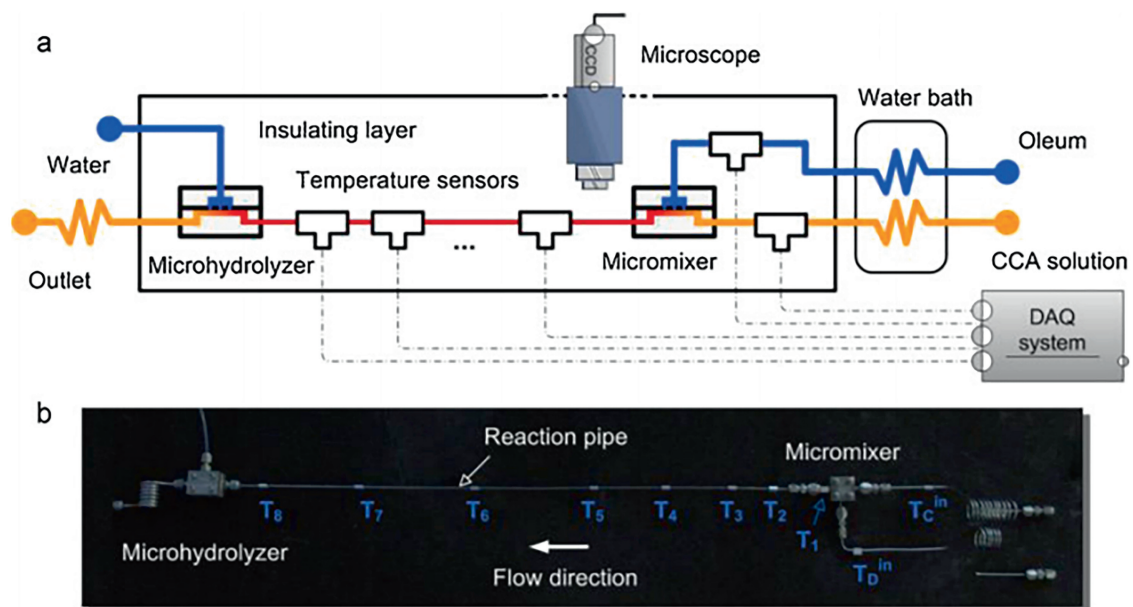
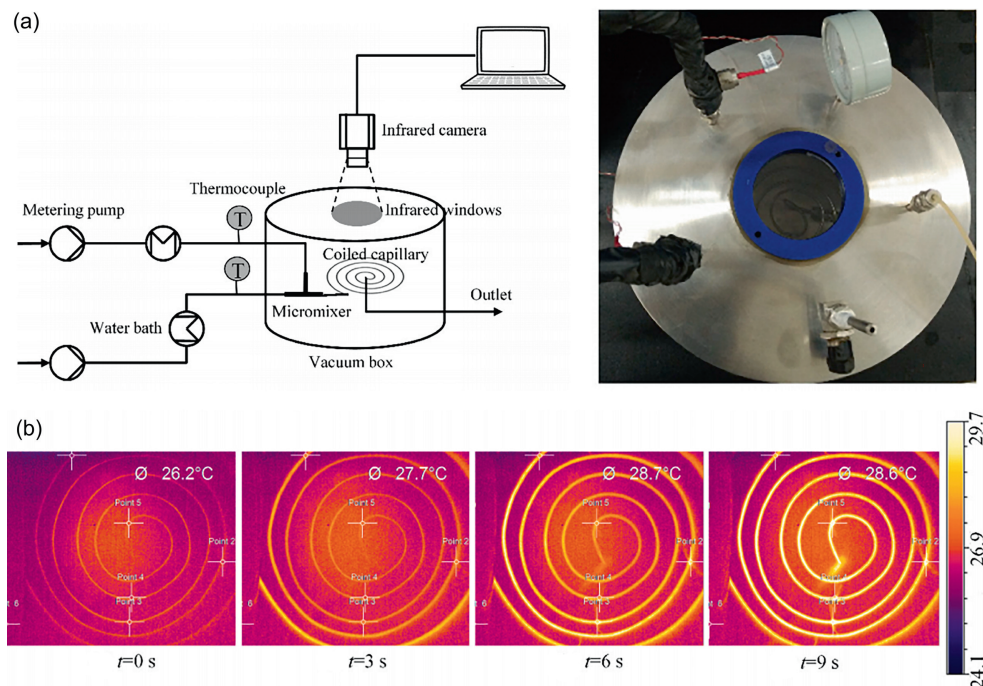
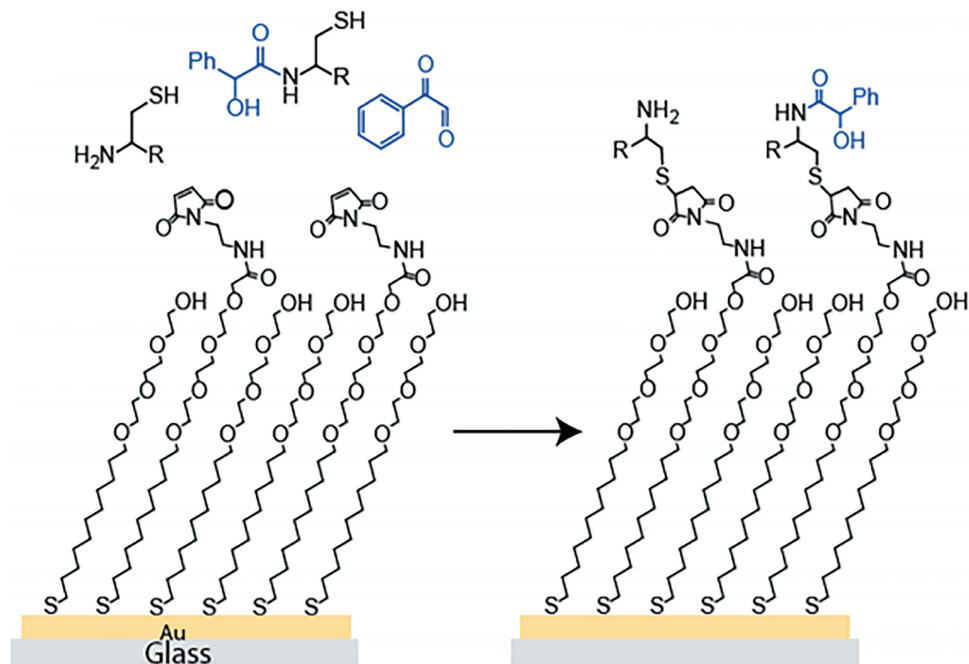


Fig. 4. Adiabatic micro-platform configuration combined with inline temperature detection. Adapted with permission of Elsevier.



**Fig. 5.** (a) The vacuum-adiabatic micro-system combined with infrared thermography for inline acquisition of reactor temperature field. (b) The typical temperature profiles at different times during measuring process. Adapted with permission of Elsevier.



**Fig. 6.** Self-assembled monolayer containing maleimide groups reacts with the cysteine-terminated peptide. Adapted with permission of American Chemical Society.

ions to catalyze the formation of nitronium ion  $\text{NO}_2^+$ , which is the electrophilic species to attack the substrate. Most of nitration processes using mixed acid as nitrating agent present a liquid–liquid heterogeneous state because the organic substrates have very limited solubility in mixed acid. It has been acknowledged that the reaction occurs at the mixed acid phase, and the mass transfer from organic phase to aqueous phase can reduce the apparent reaction rate [37]. Therefore, the reaction process is prolonged to

even several hours. Actually, nitration is a typical kind of fast and highly exothermic reactions. The intrinsic kinetics indicates that 100% conversion of aromatic substrate can be achieved with few seconds [38]. In general, the reaction heat of nitration ranges from  $-73$  to  $-253 \text{ kJ}\cdot\text{mol}^{-1}$ . Such great amount of heat release calls for the superior heat-exchange ability to control the temperature.

According to the above characteristics, the conventional batch reactor and operation mode is hard to be applied for kinetic

measurement of nitration, and the advantages of microreactors are highlighted. Table 1 summarizes the typical studies on the reaction kinetics of nitration based on microfluidic technology.

Some reactants can dissolve in the nitrating agents, forming a homogeneous reaction system, which brings convenience for kinetic measurement. Li *et al.* [38] studied the nitration of 2-ethylhexanol in mixed acid (Table 1, Entry 1). The product, 2-ethylhexyl nitrate, is a temperature-sensitive energetic substance that are highly decomposable and explosive. By using microreactors to enhance mixing and precisely control the reaction temperature and time, the conversion of 2-ethylhexanol and selectivity to 2-ethylhexyl nitrate can both exceed 99% in less than 10 seconds. Both the apparent kinetics and intrinsic kinetics were obtained in a capillary microreactor. As shown in Eq. (6), the apparent reactant rate constant,  $k_{app}$ , is a function of temperature and sulfuric concentration. The  $M_C$  function was further introduced to decouple the sulfuric concentration from the reaction rate constant, and an intrinsic kinetic equation was obtained, in which the concentration of nitrating agent is based on nitronium ion (Eq. (7)). Eventually, the activation energy  $E_a$  was determined to be  $42.7 \text{ kJ}\cdot\text{mol}^{-1}$  according to the values of  $k^0$  at different temperatures.

$$r = k_{app} C_{2-EH} C_{HNO_3} \quad (6)$$

$$r = k^0 C_{2-EH} C_{NO_2^+} 10^{-nM_C} \quad (7)$$

The nitration of acetyl guaiacol with fuming nitric acid-acetic acid system was studied by Zhang *et al.* in a capillary reactor [39]. 5-Nitroacetylguaiacol and 4-nitroacetylguaiacol were the two isomer products of this nitration process. As fuming nitric acid was greatly excess, it could be assumed that its concentration is constant. Thus, the reaction rate could be written as Eq. (8). The reaction rate constant,  $k_1$  and  $k_2$  represents the formation of the two kinds of products. According to the selectivity of the two products and the overall reaction rate at 50–90 °C,  $E_a$  were obtained respectively ( $139 \text{ kJ}\cdot\text{mol}^{-1}$  for 5-nitroacetylguaiacol,  $101 \text{ kJ}\cdot\text{mol}^{-1}$  for 4-nitroacetylguaiacol). High temperature is beneficial to improve the selectivity of targeted product, 5-nitroacetylguaiacol, because of its higher value of  $E_a$ . By improving the security of this reaction system, the microreactor enabled the process to be conducted at high temperature and high concentration of fuming nitric acid, thus elevating the selectivity.

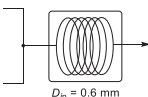
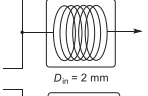
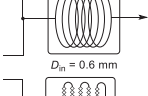
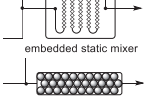
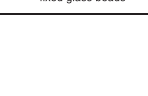
$$r = (k_1 + k_2) C_{ArH} C_{HNO_3}^0 \quad (8)$$

Rapid mixing of reactants in the initial stage of the reaction is the key to determining the intrinsic kinetics of homogeneous reactions. Theoretically, once the uniform mixing at the molecular level is achieved, mass transfer will no longer affect the reaction rate. However, the condition is totally different in heterogeneous reactions. When the two reactants or the reactant and catalyst are in different phases, the mass transfer can always affect the kinetics during the reaction. Under this condition, it is particularly important to enhance the mass transfer to eliminate its effect.

Because of the enhanced mass transfer characteristics, microfluidic technology is recognized to be an effective platform for the determination of the intrinsic kinetics of the rapid nitration under liquid–liquid heterogeneous condition. Wen *et al.* [14] studied the nitration of trifluoromethoxybenzene in a capillary microreactor using mixed acid as the nitrating agent. The set-up configuration is shown in Fig. 7, which is the typical micro-platform construction method for the determination of nitration kinetics. The mass transfer characteristics were investigated under the droplet flow condition, and the mass transfer coefficient in the acid phase was estimated using a semi-empirical equation. A quasi-homogeneous reaction kinetic model was proposed by assuming the intrinsic reaction as the rate-determining step (Table 1, Entry 3). Based on the obtained reaction constant, the Hatta number, which represents the relative speed of the reaction rate to the mass transfer rate, were further calculated. The low values of Hatta number ( $<0.3$ ) indicate that TFMB nitration was kinetically controlled, which in turn verifies the correctness of the quasi-homogeneous assumptions.

In order to further enhance the mass transfer performance, Russo *et al.* [12] developed a microreactor embedded with a static mixer (see Fig. 8). In this way, by completely eliminating the effect of mass transfer on kinetic measurement, the previously developed reaction kinetics of benzaldehyde nitration could be directly extended to the heterogeneous condition, which was in line with the practical industrial process. The kinetic results are listed in Table 1, Entry 4. This important conclusion validated that the microfluidic technology could be a promising alternative to scaled-up batch reactors for nitration process because it can achieve kinetic-control regime at a relatively low flow rate.

**Table 1**  
An overview of some typical studies on nitration kinetics

Entry	Authors	Reactants	Nitrating agent	Phase state	Kinetic equation	Activation energy/ $\text{kJ}\cdot\text{mol}^{-1}$	Microreactor scheme
1	Li, <i>et al.</i> , 2017 [38]	2-Ethylhexanol	Mixed acid	Homogeneous	$r = k^0 C_{2-EH} C_{NO_2^+} 10^{-nM_C}$	42.7	 $D_{in} = 0.6 \text{ mm}$
2	Zhang, <i>et al.</i> , 2016 [39]	Acetyl guaiacol	Fuming nitric acid & acetic acid	Homogeneous	$r = (k_1 + k_2) C_{ArH} C_{HNO_3}^0$	139 (5-nitro) 101 (4-nitro)	 $D_{in} = 2 \text{ mm}$
3	Wen, <i>et al.</i> , 2018 [14]	Trifluoromethoxybenzene	Mixed acid	Liquid–liquid	$r_i = k_i C_{TFMB}^L C_{NO_2^+} 10^{-nM_C}$	29.3 (ortho) 26.9 (para)	 $D_{in} = 0.6 \text{ mm}$
4	Russo, <i>et al.</i> , 2019 [12]	Benzaldehyde	Mixed acid	Liquid–liquid	$r_{Ni} = k_{Ni} C_{Ar}^{aq} C_{NO_2^+}$	/	 embedded static mixer
5	Lan, <i>et al.</i> , 2021 [33]	o-Dichlorobenzene	Mixed acid	Liquid–liquid	$\frac{1}{\Delta T_{max}} \frac{dT}{dt} = k C_{1,0} \left(1 - \frac{\Delta T}{\Delta T_{max}}\right) \left(M - \frac{\Delta T}{\Delta T_{max}}\right)$	31.0	 fixed glass beads

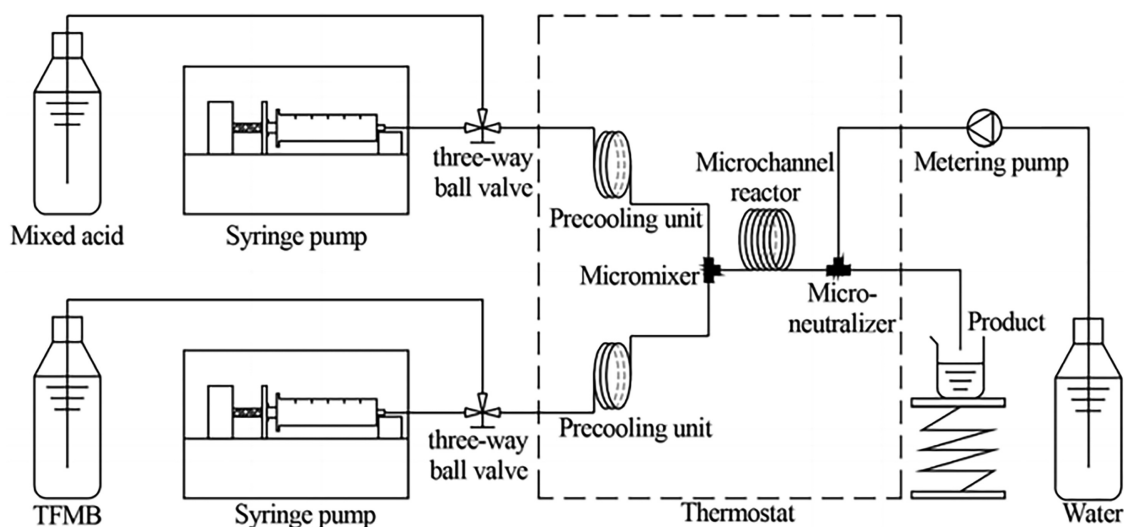


Fig. 7. Micro-platform for kinetic measurement of nitration. Adapted with permission of Royal Society of Chemistry.

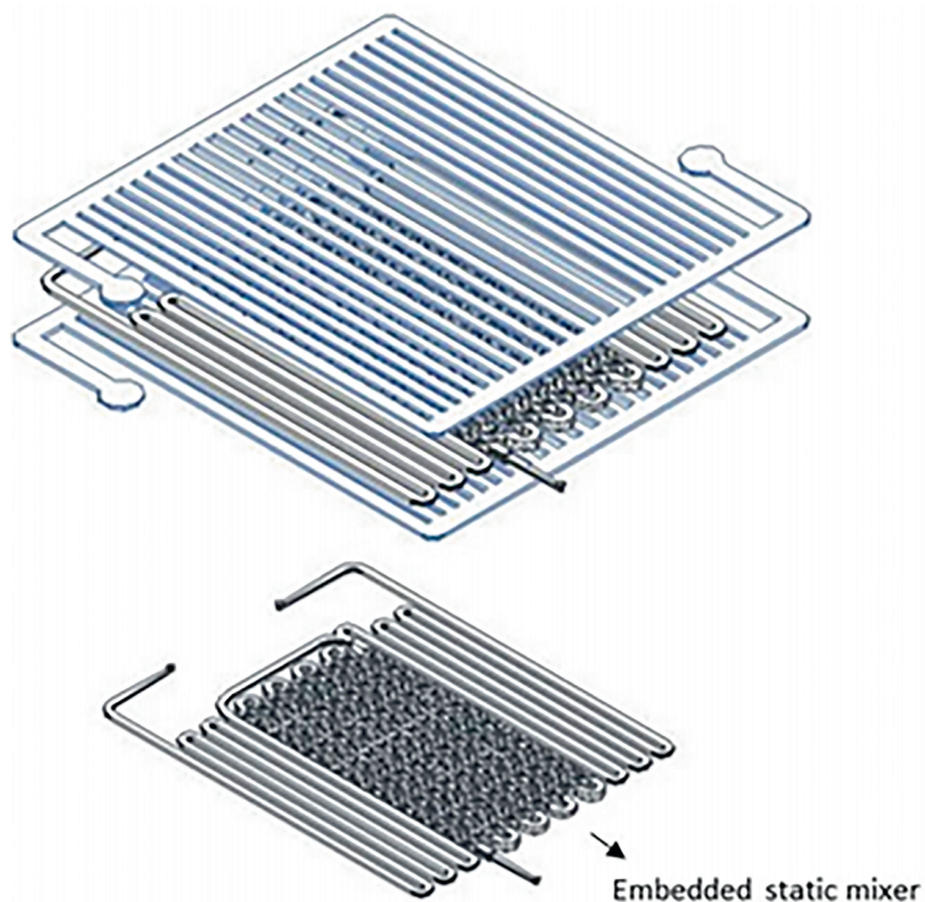


Fig. 8. Microchip embedded static mixer for mass transfer enhancement in benzaldehyde nitration process. Adapted with permission of Elsevier.

Stressed by all of the above studies, the constant temperature condition could be realized in microreactors because of the rapid heat transfer performance. However, the absolutely ideal isothermal condition is impossible to achieve even in microreactors. And the temperature gradient along the reactors can exert system error in kinetic measurement, especially for the highly exothermic

nitration completed within a few seconds. Measuring kinetics under adiabatic condition is another way that can be applied for this exothermic reaction. The basic principle behind it is to obtain the substrate conversion according to temperature rise. Lan *et al.* [33] developed an adiabatic micro-platform to investigate the continuous nitration of *o*-dichlorobenzene. As shown in Fig. 9(a), it



was demonstrated that the micropacked-bed reactor has better performances compared with capillary tubes because the fixed glass beads could enhance the mass transfer by facilitating the secondary breakage of droplets and prevent them from coalescence. Further optimizing the packing size in micropacked-bed (Fig. 9 (b)), nearly 100% conversion could be achieved within 5 seconds. Based on the second-order kinetics (Eq. (9)) and the characteristics of adiabatic reaction, the equation shown in Eq. (10) was further deduced, which is available for determination of kinetic parameter from experimental data. The fitting results can predict the substrate conversion very well (Fig. 9(c) and (d)).

$$r = -\frac{dC_1}{dt} = kC_1C_{\text{HNO}_3} \quad (9)$$

$$\frac{1}{\Delta T_{\text{max}}} \frac{dT}{dt} = A \exp(-E_a/RT) C_{1,0} \left(1 - \frac{\Delta T}{\Delta T_{\text{max}}}\right) \left(M - \frac{\Delta T}{\Delta T_{\text{max}}}\right) \quad (10)$$

### 3.2. Oxidation

Oxidation is a typical kind of highly exothermic reaction, and the extreme conditions of high temperature and high pressure are widely used for gaseous oxidation process. In most instances, pure oxygen has better oxidative performances than air [40], thus the process safety issue must be given full attention when the reaction performed in the explosion limit. The selective oxidation (e.g., selective oxidation of CO in the mixture of CO and H<sub>2</sub>) and incom-

plete oxidation (e.g., oxidation of propylene to produce propylene oxide) are preferred in many processes, where strict control of temperature is particularly important to selectivity [41]. The gaseous oxidation of small molecules is usually carried out in the presence of solid catalysts [42]. The precise measurement of gas–solid reaction kinetics is based on the rapid removal of the reaction heat to maintain constant temperature and enhancement of mass transfer to eliminate the effect of internal diffusion. In gas–liquid (hydroanthraquinone oxygen oxidation [40]) and liquid–liquid (heterogeneous oxidation using hydrogen peroxide [17]) oxidation process, the oxidant and substrate are in different phases, thus the enhancement of mass transfer between multiple phases is essential for kinetic measurement.

Microfluidic technology has been successfully applied to obtain the kinetic regularities of oxidation. Table 2 summarizes the related works in recent years, and the advantages of microreactors embodied in these studies will be introduced in the following discussion.

The preferential oxidation of CO in reformer gas (mixture of CO and H<sub>2</sub>) is a promising method for reducing CO contamination down to  $5 \times 10^{-3}$  % (volume), and the prepared high-purity hydrogen can be used as energy source in fuel cells. Han *et al.* [28] developed a micropacked-bed reactor with fixed Ru/ $\gamma$ -Al<sub>2</sub>O<sub>3</sub> catalyst to study the preferential oxidation of CO at atmospheric pressure and temperature range of 50–300 °C. Combined with the inline analysis method of gas chromatography, the experimental results were rapidly recorded. The effects of partial pressure of CO and O<sub>2</sub>, as

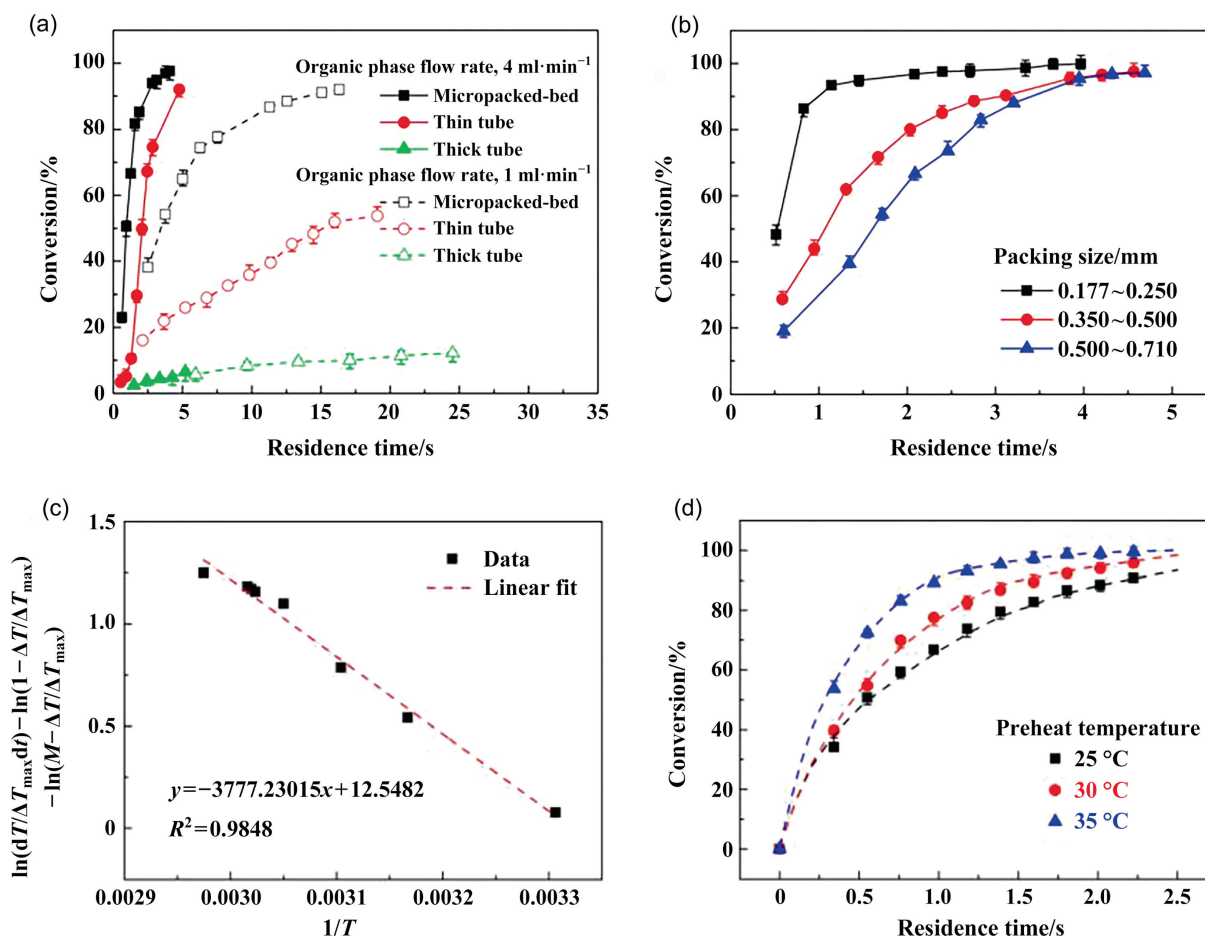
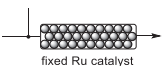
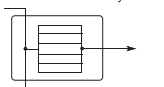
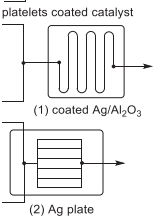
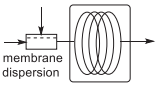
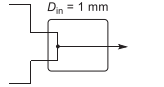
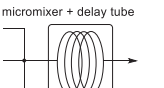
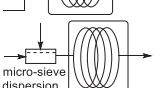
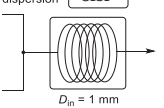


Fig. 9. (a) Time profiles of conversion under adiabatic conditions in different forms of microreactors. (b) Reaction performances of micropacked-bed reactors with different packing sizes. (c) Fitting results of adiabatic kinetic model with experimental data. (d) Prediction of the isothermal nitration by the obtained kinetic model under different temperatures. Adapted with permission of Springer.

**Table 2**  
An overview of some typical studies on oxidation kinetics

Entry	Authors	Reactants	Catalyst	Phase state	Kinetic equation	Activation energy /kJ·mol <sup>-1</sup>	Microreactor scheme
1	Han, <i>et al.</i> , 2001 [28]	CO, O <sub>2</sub>	Ru/γ-Al <sub>2</sub> O <sub>3</sub>	Gas–solid	$r = kP_{CO}^{-0.48} p_{O_2}^{0.85}$	95	
2	Nikolaidis, <i>et al.</i> , 2016 [43]	CO, O <sub>2</sub>	Pt-Ru/γ-Al <sub>2</sub> O <sub>3</sub>	Gas–solid	$r = kP_{CO}^{-0.53} p_{O_2}^{0.79}$	94.2	
3	Russo, <i>et al.</i> , 2015 [44]	ethylene, O <sub>2</sub>	Ag	Gas–solid	$r = \frac{k_1 C_E C_{O_2}}{(1 + K_E C_E + K_{O_2} C_{O_2})^2}$	31.0 (silver plate) 45.9 (washcoat)	
4	Tan, <i>et al.</i> , 2011 [40]	THEAQH <sub>2</sub> , O <sub>2</sub>	/	Gas–liquid	$r = kC_{THEAQH_2} C_{O_2}^L$	56.8	
5	Ebrahimi, <i>et al.</i> , 2012 [45]	Formic acid, H <sub>2</sub> O <sub>2</sub>	Sulfuric acid	Homogeneous	$r = \frac{dC_{FA}}{dt} = -kC_{HP}C_{FA}C_{H_2O} + k^{-1}C_{PFA}C_W C_{H_2O} +$	60.4 (forward) 63.6 (reverse)	
6	Zhao, <i>et al.</i> , 2021 [46]	Benzene, H <sub>2</sub> O <sub>2</sub>	Sodium metavanadate	Gas–liquid	$\frac{dC_{ben}}{dt} = -k_1 C_{ben} C_{H_2O_2}$	99.5	
7	Dong, <i>et al.</i> , 2015 [17]	Cyclohexanone, NH <sub>3</sub> ·H <sub>2</sub> O, H <sub>2</sub> O <sub>2</sub>	TS-1	Liquid–solid	$\frac{dC_{ben}}{dt} = -k_1 C_{ben} C_{H_2O_2}$	93.2	
8	Li, <i>et al.</i> , 2020 [47]	Cyclohexanol, cyclohexanone, HNO <sub>3</sub>	Cu(II), V(V)	Liquid–liquid → gas–liquid–liquid	$r_1 = \frac{dC_1}{dt} = kC_{NA}^\alpha C_{IM}^\beta$	94.0 (AA) 103 (GA) 64.2 (SA)	

well as temperature on the reaction rate were analyzed respectively to obtain the reaction orders of reactants and the activation energy. Entry 1 in Table 2 shows the obtained kinetic equation and the value of apparent activation energy based on power law. The negative value of CO order and positive value of O<sub>2</sub> indicate that the reaction is limited by the adsorption of dissociative O<sub>2</sub> molecules on the catalyst surface due to the presence of a dense CO layer on it, which is also the essence of selective oxidation even if the partial pressure of CO is much lower than H<sub>2</sub>. It was also demonstrated that Ru/γ-Al<sub>2</sub>O<sub>3</sub> catalyst exhibited better performances than the commonly used Pt supported catalyst, with respect to higher activity and selectivity over a wide range of CO concentrations.

The plug flow (PFR) model is always used to establish mass balance equation in microreactors. However, the velocity distribution exists in the radial direction of the tube or the microchannel, leading to the fact that the residence time distribution (RTD) does not perfectly comply to the PFR model. Nikolaidis *et al.* [43] established a micro-structured recycle reactor, relying on the large recycle ratio to simulate the operation mode of CSTR in a microreactor. The RTD results of the recycle reactor justifies the assumption that the recycle loop behaves as an ideally mixed CSTR (see Fig. 10). On this platform, the kinetics of CO selective oxidation was studied. The reaction kinetics of pure CO with O<sub>2</sub> catalyzed by Pt-Ru/γ-Al<sub>2</sub>O<sub>3</sub> was measured first. And then, the kinetics under the influence of H<sub>2</sub>, CO<sub>2</sub>, and H<sub>2</sub>O was studied to uncover the mechanism of CO preferential oxidation. The detailed kinetic results, which are listed in Table 2 (Entry 2), are basically consistent with the study of Entry 1. The oxidation of CO is also an important reaction

for automobile exhaust treatment, which was studied in a fix-bed microreactor to obtain the intrinsic kinetics [42].

The above studies don't involve the effect of internal mass transfer on the reaction kinetics. Considering the intrinsic reaction kinetics and internal diffusion to describe the epoxidation of ethylene, Russo *et al.* [44] developed two novel reactor models, one for a washcoated reactor and the other one for a silver plate microreactor. The kinetic parameters were obtained by fitting the two models to experimental data. As shown in Table 2 (Entry 3), the differences of kinetic parameters including activation energy and adsorption equilibrium constant for the two reactors indicated that the loading method of the catalyst and the flow characteristics in the reactor can affect the reaction kinetics.

The reaction kinetics of propylene epoxidation over Au/TiO<sub>2</sub> catalyst was studied in a stainless-steel capillary microreactor (0.9 mm inner diameter) packed with 20 mg catalyst [48]. The kinetic model containing the catalyst deactivation process were established to quantitatively explain the effect of concentrations of hydrogen, oxygen and propylene on the yield of propylene oxide. The experiments under the condition within explosion limit were safely carried out in microreactors, thus broadening the measurable concentration ranges.

The oxychlorination of ethylene to prepare dichloroethane over CuCl<sub>2</sub> catalyst was studied in two kinds of microreactors, the first one was with catalyst coated on the walls, and the second one was with catalyst pellets packed in it [49]. A higher reaction rate was achieved in the first microreactor because the higher internal surface-to-volume ratio was realized by establishing a thinner catalyst layer. The activation energy was measured in both of the two

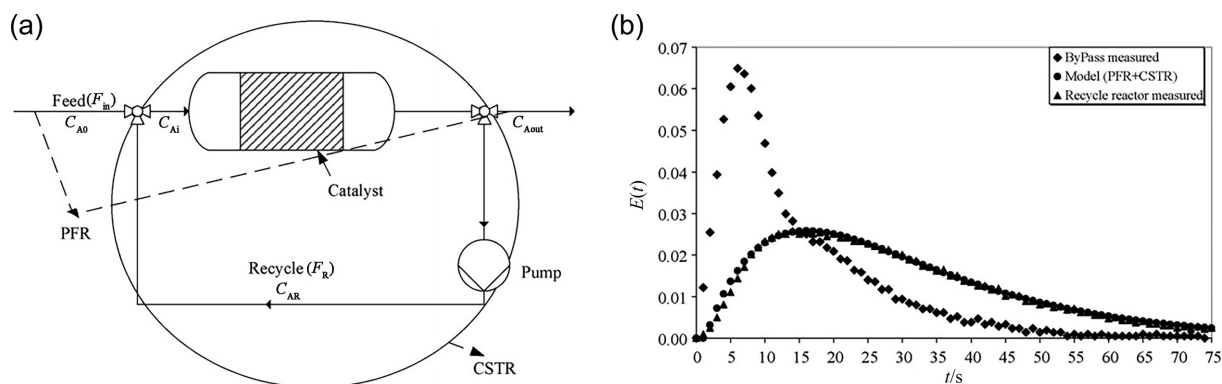


Fig. 10. (a) Process diagram of the recycle microreactor. (b) Residence time distribution in the recycle reactor at recycle ratio of 35. Adapted with permission of Elsevier.

reactors ( $49.0 \text{ kJ}\cdot\text{mol}^{-1}$  in the first one, and  $36.2 \text{ kJ}\cdot\text{mol}^{-1}$  in the second one). It is understandable that the activation energy was higher in the first microreactor because the internal mass transfer was further enhanced and the overall reaction was closer to the kinetic-control condition.

When the substrate is liquid under the applied temperature and pressure conditions, the reaction system of oxygen oxidation is transformed to gas–liquid or gas–liquid–solid phase state, and the mass transfer between gas and liquid phases should be considered during kinetic measurement. Tan *et al.* [40] developed a membrane-dispersion microreactor and used it for oxidation of hydrogenated 2-ethyltetrahydroanthraquinone, which is an essential step for  $\text{H}_2\text{O}_2$  production (see Fig. 11). The size of the dispersed bubbles was around  $100 \mu\text{m}$ , which was only one-fifth to one-tenth of that in the conventional equipment. Accordingly, the Hatta number was calculated to be 0.01–0.2, thus the oxidation process was proved to be kinetic control based on the enhancement of mass transfer. The intrinsic reaction kinetics using pure oxygen and air as oxidant was studied respectively, the obtained results are listed in Table 2 (Entry 4). The reaction rate using pure oxygen is obviously faster, but the safety problem will be more prominent.

The oxygen oxidation of benzyl alcohol was studied in a flat membrane microchannel reactor packed with  $\text{Ru}/\text{Al}_2\text{O}_3$  catalyst [50]. It was proved that the mass transfer of oxygen in the catalyst bed is the rate-control step, thus the key to process intensification was to reduce the reactor depth.

Hydrogen peroxide is a green oxidant, and the reaction conditions are usually milder than oxygen oxidation [7]. Ebrahimi *et al.* [45] studied the peroxidation of formic acid and acetic acid

catalyzed by sulfuric acid in a tubular microreactor. The Peclet number was higher than 500 in this reaction system, which meant that the axial dispersion was negligible. However, the velocity maldistribution and mass diffusion in radial direction could influence the kinetic measurement. Three models, which were respectively based on PFR (1), laminar flow (parabolic velocity distribution) considering the radial diffusion (2) or not (3), were established and fitted with the experimental data. The results demonstrated that model (3) had the best fit, indicating that considering the velocity distribution under laminar flow was beneficial to improve the accuracy of kinetic model (the results are shown in Table 2 entry 5). The maldistribution of velocity in laminar flow can broaden the RTD of reactor. The use of helical capillary to replace the straight one is an effective solution because a secondary flow could be formed by Dean Vortices in the helical capillary microreactor [51], which was used for kinetic measurement of propionic acid peroxidation [52].

Another case using hydrogen peroxide as the oxidant is the direct oxidation of benzene to phenol with sodium metavanadate as the catalyst [46]. In a tubular microreactor, the actual residence time was obviously shorter than the set one because the gas phase was formed from the decomposition of  $\text{H}_2\text{O}_2$ . By fitting the flow velocity of gas phase along the reaction tube, the residence time was calculated accurately. In this way, the reaction kinetics of phenol synthesis, hydrogen peroxide decomposition and *p*-benzoquinone formation were determined together. The results are listed in Table 2 (Entry 6).

TS-1 is a commonly used solid catalyst in hydrogen peroxide oxidation process. Dong *et al.* [17] developed a micro-platform to

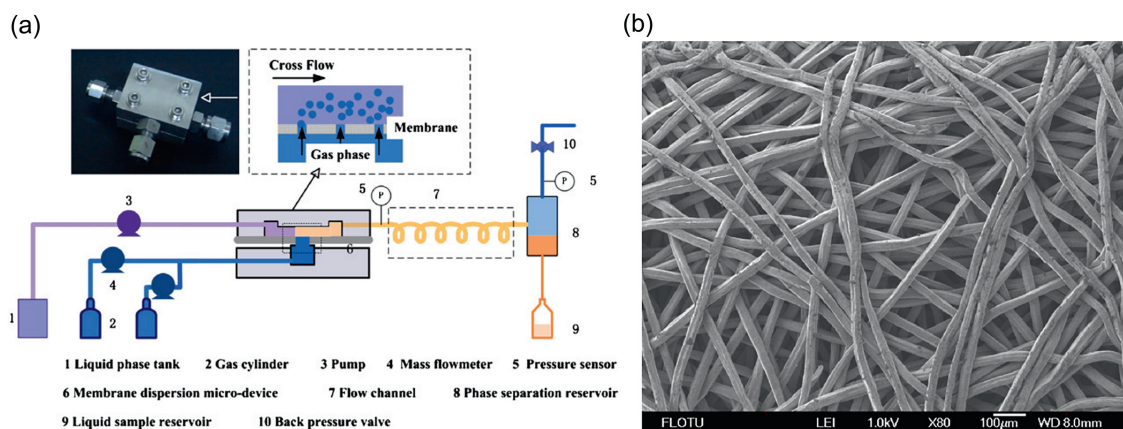


Fig. 11. (a) Set-up of oxidation of hydrogenated 2-ethyltetrahydroanthraquinone using membrane-dispersion microreactor (b) The SEM picture of the microfiltration membrane surface. Adapted with permission of Elsevier.

determine the reaction kinetics of cyclohexanone ammoximation reaction in the slurry-flow condition. To obtain the intrinsic kinetic laws, the effect of external diffusion resistance was eliminated by the enhanced mixing and rapid mass transfer in the microreactor, and the effect of internal diffusion was eliminated by reducing the particle size of catalyst. Moreover, an ultrasonic field was introduced to avoid the sedimentation of solid catalyst. By assuming that the reaction of the hydrogen peroxide adsorbed on Ti active sites with free ammonia was the rate-determining step, the intrinsic kinetic model was established and fitted well with the experimental results (shown in Table 2, Entry 7).

Except for oxygen and hydrogen peroxide, nitric acid can also be used as the oxidant in the presence of copper and vanadium catalysts. Li *et al.* [47] studied the oxidation of cyclohexanol and cyclohexanone (K/A oil) with nitric acid to produce adipic acid. This reaction is accompanied by the formation of gaseous by-product  $\text{NO}_x$ , so the phase state changed from liquid-liquid to gas-liquid-liquid and the apparent flow velocity increased as the reaction proceeded. By measuring the volumetric flow rate of the gas mixture at different length of capillary microreactor, the residence time was calculated by integration based on the assumption that the flow velocities of gas phase and liquid phase were the same. The apparent power-law kinetic model was established as shown in Eq. (11), NA represents nitric acid, IM represents the reaction intermediates, and the subscript “*i*” respectively represents three different products, adipic acid, glutaric acid and succinic acid. The activation energy in the formation of the three products were obtained and the results are listed in Table 2 (Entry 8). The activation energy of adipic acid, which is the targeted product, is in the middle of the three products. This fact determines that temperature must be strictly controlled to improve selectivity for this highly exothermic reaction, and the advantage of rapid heat exchange in microreactors is embodied here.

$$r_i = \frac{dC_i}{dt} = k_0 \exp(-E_a/RT) C_{\text{NA}}^\alpha C_{\text{IM}}^\beta \quad (11)$$

Microfluidic technology can also be used to measure the intrinsic kinetics of biocatalytic oxidation [53]. The obtained maximum reaction rate (kinetic parameter  $V_{\text{max}}$  in Michaelis-Menten equation) in the microchip reactor ( $197 \text{ U} \cdot \text{mg}^{-1}$ ) was nearly 30 times higher than that measured in a cuvette ( $6.76 \text{ U} \cdot \text{mg}^{-1}$ ), which is also due to the rapid mass transfer coefficient and high surface-to-volume ratio.

### 3.3. Hydrogenation

Hydrogen is usually used as the hydrogen source in hydrogenation, and transition metals (such as Co, Ni, Pd, Ru and so on) are the most commonly used catalysts. According to the phase state (gas or liquid) of the substrate under the applied reaction conditions, the gas-solid or gas-liquid-solid reaction system can be formed in hydrogenation. In order to improve the reaction rate, high pressure (0.5–10 MPa) is usually needed to increase the partial pressure of  $\text{H}_2$  in gas phase (for gas-solid hydrogenation) or its solubility in liquid phase (for gas-liquid-solid hydrogenation). Moreover, the pretty high temperature is also required in some reactions (e.g.,  $>500 \text{ K}$  for CO hydrogenation [54] and phenol hydrogenation [55]). Such extreme reaction conditions make the safety problem to be the first element. In order to obtain the kinetic regularities of hydrogenation to guide the design of reactors and processes, the steady flow condition and narrow RTD are the basis [5]. Besides, the mass transfer enhancement between multiple phases and strictly control of temperature under high exothermic condition also seem to be very important [56]. Under the constraints of these characteristics, the measurement of intrinsic kinetics of hydrogenation is still difficult. In recent years, microflu-

idic technology has been acknowledged as a strong tool to solve these problems, and the related studies are listed in Table 3.

Hydrogenation of carbon monoxide with  $\text{H}_2$ , also known as Fischer-Tropsch (F-T) process, is a very important reaction in petrochemical industry to produce a wide range of hydrocarbon products, including light olefins and long-chain hydrocarbons (fuels) (see Fig. 12) [61]. Transitional metals are considered to be active catalysts for F-T process. Among them, cobalt and iron have been widely used in industry because of their affordable price and high activity under relative moderate reaction conditions. Mirzaei *et al.* [54] studied the kinetics of F-T process using Fe-Co-Mn/MgO catalyst prepared by sol-gel method in a fixed bed micro-reactor. Eighteen possible mechanisms were put forward based on Langmuir-Hinshelwood-Hougen-Watson theory, and the differences were reflected in various adsorption forms on the catalyst surface and carbon chain distribution pathways. Furthermore, the corresponding kinetic equations were deduced according to different possible rate-determining steps. Fitting the parameters in the obtained kinetic equation with experimental data and analyzing the errors via rigorous mathematical methods, finally the kinetic model shown in Eq. (12) was proved to be the best one, and the activation energy was calculated to be  $110.9 \text{ kJ} \cdot \text{mol}^{-1}$ . One significant problem in this study is that it is not sufficient to judge whether the F-T reaction is controlled by internal diffusion or kinetics just by the magnitude of activation energy. Therefore, the authors further eliminated the effect of internal diffusion by reducing the catalyst particle size in the following study [57]. Using the similar experimental and analytical methods but different catalyst preparation methods, the kinetic equations and activation energies were determined in the presence of Fe-Co-Ni supported catalyst [57] and Fe-Mn catalyst [58] (results are listed in Table 3, Entries 2 and 3).

$$-r_{\text{CO}} = \frac{k_p b_{\text{CO}} b_{\text{H}_2} P_{\text{CO}} P_{\text{H}_2}}{(1 + 2(b_{\text{CO}} P_{\text{CO}})^{0.5} + b_{\text{H}_2} P_{\text{H}_2})^3} \quad (12)$$

Extremely high temperature is needed for gas-solid hydrogenation of substances with high boiling points. Mahata *et al.* [55] studied the kinetics of phenol hydrogenation to cyclohexanone in a tubular microreactor packed with Pd/MgO catalyst under atmospheric pressure and temperature range of 473 to 563 K. As shown in Eq. (13), the apparent power-law kinetic model was used, and the fitting results indicated that the order of phenol increased from  $-0.53$  to  $0.46$  as the temperature rose from 473 K to 563 K. This fact suggested the weaker adsorption on the catalyst surface at higher temperature. The similar conclusion was also obtained by Vishwanathan *et al.* [62] in the study of gas-solid hydrogenation of *o*-chloronitrobenzene. As the temperature went up from 523 K to 583 K, the reaction order of *o*-chloronitrobenzene increased from 0.39 to 1.45.

$$r = k P_{\text{phenol}}^\alpha P_{\text{H}_2}^\beta \quad (13)$$

The variation of reaction orders with temperature indicates that the simple power law equation model doesn't fit well in gas-solid phenol hydrogenation. Massoth *et al.* [63] developed a kinetic model based on Langmuir-Hinshelwood method to describe the hydrogenation of different methyl-substituted phenols (one to three methyl groups substituted at different positions on the benzene ring). The effects of substituted methyl groups, with respect to their numbers and locations, on the adsorption and reaction rate constants were systematically studied. The proposed hydrogenation mechanism is shown in Fig. 13. Two different reaction pathways led to the formation of methyl-substituted benzene and cyclohexane respectively. Combined with quantum chemistry calculation, it was demonstrated that the adsorption constant and

**Table 3**  
An overview of some typical studies on hydrogenation kinetics

Entry	Authors	Reactants	Catalyst	Phase state	Kinetic equation	Activation energy / $\text{kJ}\cdot\text{mol}^{-1}$	Microreactor scheme
1	Mirzaei, et al., 2013 [54]	CO, H <sub>2</sub>	Fe–Co–Mn/MgO	Gas–solid	$-r_{\text{CO}} = \frac{k_p b_{\text{CO}} b_{\text{H}_2} P_{\text{CO}} P_{\text{H}_2}}{(1 + 2(b_{\text{CO}} P_{\text{CO}})^{0.5} + b_{\text{H}_2} P_{\text{H}_2})^3}$	111	
2	Mirzaei, et al., 2014 [57]	CO, H <sub>2</sub>	Fe–Co–Ni	Gas–solid	$-r_{\text{CO}} = \frac{k b_{\text{CO}} P_{\text{CO}} (b_{\text{H}_2} P_{\text{H}_2})^{1/2}}{(1 + b_{\text{CO}} P_{\text{CO}} + (b_{\text{H}_2} P_{\text{H}_2})^{1/2})^2}$	82.2	
3	Mirzaei, et al., 2015 [58]	CO, H <sub>2</sub> , H <sub>2</sub> O	Fe–Mn	Gas–solid	$-r_{\text{CO}} = \frac{K P_{\text{CO}}}{(1 + 2(\alpha P_{\text{CO}})^{0.5} + (\beta P_{\text{H}_2})^{0.5})^2}$	105	
4	Mahata, et al., 1997 [55]	Phenol, H <sub>2</sub>	Pd/MgO	gas–liquid	$r = k P_{\text{phenol}}^x P_{\text{H}_2}^y$ Orders changed with temperature	63	
5	Joshi, et al., 2013 [56]	4 propylguaicol, H <sub>2</sub> , H <sub>2</sub> O	Ni–Mo/Al <sub>2</sub> O <sub>3</sub>	Gas–liquid–solid	$r = \frac{k(K_{\text{H}_2} C_{\text{H}_2})(K_{\text{RC}} C_{\text{RC}})}{(1 + K_{\text{RC}} C_{\text{RC}})[1 + (K_{\text{H}_2} C_{\text{H}_2})^{1/2}]^2}$	33.9	
6	Tanimu, et al., 2018 [59]	Phenylacetylene, H <sub>2</sub>	Pd/CeO <sub>2</sub>	Gas–liquid–solid	$r = k C_{\text{PG}}^{0.6}$	41.4	
7	Maresz, et al., 2020 [60]	Cyclohexanone, n-butanol	Zirconium–silica	Liquid–solid	$r = k C_{\text{CH}}$	54	

(1) Alkane production:



(2) Alkene production:



(3) Water-gas shift reaction:

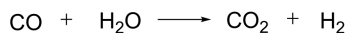


**Fig. 12.** The main representative reactions in F-T process.

intrinsic reaction rate constants of the two pathways were related to the electrostatic potential and ionization potentials of certain valence molecular orbitals of the substituted phenols.

Supercritical fluids are a kind of novel and green reaction media because of their great solvent power and excellent mass and heat transfer performances [64]. Using supercritical propylene as the reaction media, the hydrogenation process of sunflower oil and its kinetic regularities were studied in a packed-bed (Pd/C) microreactor under the conditions of 20 MPa, 428–488 K [65]. Compared with the traditional gas–liquid–solid slurry operation in batch reactors, the reaction was greatly intensified by forming a homogeneous vapor phase in supercritical media, in which the mass transport resistance was alleviated and the actual concentration of H<sub>2</sub> on the catalyst surface was elevated.

When the substrate is in liquid state under the applied hydrogenation conditions, the reaction system will contain gas, liquid and solid three phases. Under this condition, the complex mass transfer processes, including gas–liquid mass transfer, external and internal liquid–solid mass transfer will significantly reduce the apparent reaction rate and exert great influence on the measurement of intrinsic kinetics. The conventional gas–liquid–solid (e.g., batch, packed bed, slurry) reactors cannot perform stable flow state and greatly enhanced the mass and heat transfer performances because of the limited surface-to-volume ratio and small transfer coefficients [5]. As a strong tool to enhance the mass transfer between multiple phases, microreactors are applied to obtain the intrinsic kinetics of hydrogenation in gas–liquid–solid reaction system.

Joshi *et al.* [56] studied the hydrodeoxygenation of 4 propylguaicol using Ni–Mo/Al<sub>2</sub>O<sub>3</sub> catalyst in a micropacked-bed reactor. By increasing the superficial velocity to 2.5 m·s<sup>-1</sup> and reducing the catalyst particle size to 75–150 μm, the effects of external and internal mass transfer on the reaction rate could be neglected. Using Langmuir – Hinshelwood approach, a series of intrinsic kinetic equations were deduced according to different adsorption mechanisms and rate-determining steps. And it was found that the kinetic model, which was derived based on the surface reaction as the rate-controlling step and noncompetitive adsorption of reactants and nondissociative adsorption of hydrogen, was the best one to fit the experimental data. The specific results are listed in Table 3 (Entry 5).

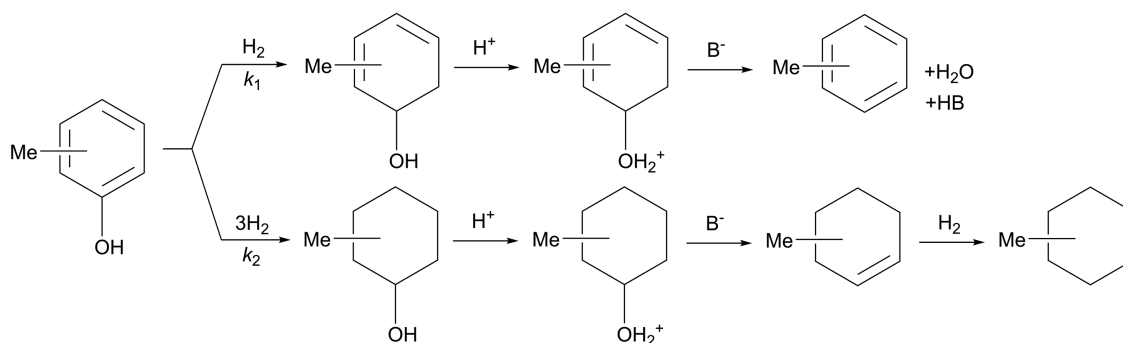


**Fig. 13.** The proposed two reaction pathways of hydrogenation of methyl-substituted phenols.

Hydrogenation of levulinic acid to  $\gamma$ -valerolactone was also studied in a micropacked-bed reactor using Ru/C catalyst [5]. A rigorous kinetic model was developed, considering the surface reaction and complete mass transfer processes between multiple phases. However, the obtained results indicated that the hydrogenation process was limited by external liquid–solid mass transfer of the dissolved  $H_2$  under the majority of operating conditions (70–130 °C and 0.9–1.5 MPa). Therefore, the microdevice and operation conditions should be further optimized, for example, by elevating the gas phase ratio to reduce the thickness of liquid film on catalyst surface.

Except for micropacked-bed reactor, the microchannel with catalyst coating on the walls is another kind of microreactor with immobilized solid catalyst. The comparisons between these two kinds of microreactors have been introduced in the previous review article [7]. Tanimu *et al.* [59] developed a capillary microreactor, its inner walls were covered by the ceria thin film, which was used as a catalyst support for palladium nanoparticles. The constructed microreactor was applied in the phenylacetylene hydrogenation to prepare styrene. It was proved that the external diffusion resistance could be neglected according to Mears' criterion ( $C_m = \frac{-r_A \rho R m}{k_c C_o} = 0.0469 < 0.15$ ). And internal diffusion resistance could also be neglected because the thickness of Pd/CeO<sub>2</sub> film was only 200 nm, and this is exactly the advantage of washcoated microreactors. The obtained kinetic results are listed in Table 3 (Entry 6).

Also used in the hydrogenation of phenylacetylene, another construction method of washcoated capillary microreactor was proposed by Rebrov *et al.* [66]. The Pd nanoparticles were directly incorporated into the mesoporous titania matrix and delivered to the internal surface of a fused silica capillary. It was demonstrated that the catalytic walls prepared in this way were more stable and the catalytic performances reached close to those obtained with a homogeneous Pd catalyst.

Except for molecular hydrogen, alcohols can also be used as hydrogen donors. Maresz *et al.* [60] studied the reduction of cyclohexanone with n-butanol to produce cyclohexanol in three types of zirconium-silica monolithic microreactors with different pore structures in both the nanometric and micrometric scales. Highest reaction rate was obtained in the most compact monolithic microreactor with the smallest pore structure, however, the pressure drop was also the highest. The obtained apparent kinetic results are listed in Table 3 (Entry 7).

### 3.4. Photochemical reaction

Photochemical reactions have been widely used in organic synthesis and pollutant treatment [67]. Different from thermochemical activation, photons are utilized to provide sufficient energy to overcome the activation energy in photochemical reactions. Based on different activation pathways, photochemical reactions can be divided into direct and indirect excitations. The direct excitation pathway requires the reactant molecules to have chromophoric moiety to absorb energy of photons. The indirect excitation pathway requires the participation of photocatalyst or photosensitizer, which can absorb light energy and pass it to reactant molecules in the form of electron energy that is available for subsequent chemical transformation [68].

The intrinsic kinetics is the basis to design or scale up a photochemical reactor. How to obtain a uniform and controllable light intensity distribution in the reactor is the key to kinetics determination. According to Bouguer-Lambert-Beer law, it is difficult to realize a homogeneous irradiation inside a conventional batch reactor because of its large characteristic dimension. Besides, the insufficient mixing and relatively low rate of mass transfer can

make the reaction controlled by external or internal diffusion, and this effect can be more obvious for fast photochemical reactions with multiple phases. All of the above limitations can be alleviated to some degree by utilizing microfluidic technology. Table 4 summarizes the typical works about the kinetic studies of photochemical reaction in microreactors, whose advantages will be illustrated with specific examples in the following discussion.

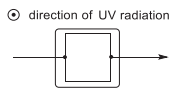
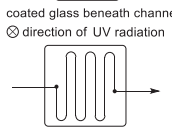
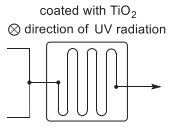
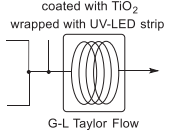
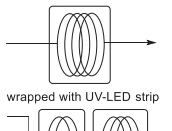
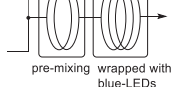
As a semiconductor material, TiO<sub>2</sub> nanoparticle has been proved to be one of the most efficient photocatalyst because of its band-gap energy of 3.0–3.2 eV [67]. Activated by photons, the formed electrons ( $e^-$ ) and holes ( $h^+$ ) constitute an oxidation–reduction system and interact with H<sub>2</sub>O and dissolved oxygen to generate highly reactive free radicals, which can be further utilized to oxidize and degrade the substrates [72]. Because the external light is supposed to uniformly irradiate on the catalyst surface, the washcoated microreactor is more beneficial than micropacked-bed reactor. Padoin *et al.* [16] developed a glass microfluidic chip with TiO<sub>2</sub> nanoparticles (TiO<sub>2</sub>-P25) and a synthesized composite TiO<sub>2</sub>-graphene catalyst immobilized on the inner walls, and used it to study the degradation of methylene blue. Computational simulations were carried out to exhibit the light distribution at the photocatalyst layers. The obtained simulation results (shown in Fig. 14) indicated that the entire film was exposed to approximately the same light intensity conditions, which was attributed to the short light penetration depth in microchannels.

Another limitation for intrinsic kinetic measurement is the external and internal mass transfer resistance existing in the heterogeneous catalytic system. Satuf *et al.* [69] established a detachable photocatalytic microreactor and systematically studied the flow characteristics, external and internal mass transfer rate, as well as radiation distribution in it. As shown in Table 5, the residence time, diffusion time (both in the fluid and catalyst pores) and reaction time were calculated respectively, and according to the relative size of them, the dimensionless numbers of  $Pe$ ,  $Da_I$ ,  $Da_{II}$ , and  $\phi$  (Thiele modulus) were obtained to estimate the reactant conversion rate and to judge whether the reaction was controlled by mass transfer or by intrinsic kinetics. According to the study of Aillet *et al.* [73], the criterion was provided in Fig. 15. By adjusting the flow rate and geometry of microreactors to make the operation condition located in the range of kinetic-control, the intrinsic kinetic model of degradation of clofibrilic acid was developed and fitted well with experimental data (listed in Table 4, Entry 1) [69].

Krivec *et al.* [18] studied the photocatalytic treatment process of phenol wastewater in a TiO<sub>2</sub> immobilized microreactor (Table 4, Entry 2). A three-dimensional mathematical model including mass diffusion and intrinsic reaction kinetics was established under the laminar flow condition. According to the calculated Thiele modulus ( $<6 \times 10^{-4}$ ) and Péclet number ( $>240$ ), it was demonstrated that the effects of external and internal diffusion were negligible, and the intrinsic kinetics and convection played the dominant roles. The effects of light intensity and pH on the reaction rate was systematically studied. The experimental results at different UV intensities did not display any observable intensity-related effect, which meant that the obtained kinetic parameters were presented under saturated light condition. In contrast, the value of pH significantly influenced the reaction kinetics by affecting the charge properties on the photocatalyst surface and the interaction with reactant molecules. Meanwhile, under high pH condition, the photocatalytic reaction can be enhanced by the participation of oxidative hydroxyl, which was generated from hydroxide ions.

The above oxidative degradation process was performed in liquid–solid state, Yu and Wang [70] further enhanced the reaction by introducing a gas phase, forming a gas–liquid Taylor flow in the microchannel (Table 4, Entry 3). As shown in Fig. 16, the introduced gas bubble can facilitate the surface refresh by taking away

**Table 4**  
An overview of some typical studies on photochemical reaction kinetics

Entry	Authors	Reactants	Catalyst (photosensitizer)	Phase state	Kinetic equation	Activation energy / $\text{kJ}\cdot\text{mol}^{-1}$	Microreactor scheme
1	Satuf, et al., 2019 [69]	Clofibrac acid	$\text{TiO}_2$	Liquid–solid	$r = k \frac{A_{\text{cat}}}{V_{\text{T}}} ((e_{\text{r}}^{a,s})_{A_{\text{cat}}})^{0.5} C$	/	
2	Krivec, et al., 2015 [18]	Phenol	$\text{TiO}_2$	Liquid–solid	$r = \frac{\sum_{j=1}^n (\pm \eta_j k_j C_j)}{1 + \sum_{k=1}^m K_k C_k} I^n$	/	
3	Yu and Wang, 2020 [70]	Methylene blue, $\text{O}_2$	$\text{TiO}_2$	Gas–liquid–solid	$r = k_{\text{app}} C$	/	
4	Su, et al., 2015 [68]	Thiophenol, $\text{O}_2$	Eosin Y	Gas–liquid	$r = k_0 q^{0.56} \varphi^{0.21} C_{\text{sub}} C_{\text{O}_2}^2$	/	
5	Shen, et al., 2019 [10]	Norbornadiene	Triplet-photosensitizer, EMK	Homogeneous	$r = K_{\text{f}} C_{\text{NBD}}$ $K_{\text{f}} \propto I_0$	/	
6	Shi, et al., 2021 [71]	Benzene, DDQ, $\text{H}_2\text{O}$	DDQ	Homogeneous	$\frac{dC_{\text{phenol}}}{dt} = k C_{\text{ben}}^2 C_{\text{DDQ}}$	/	

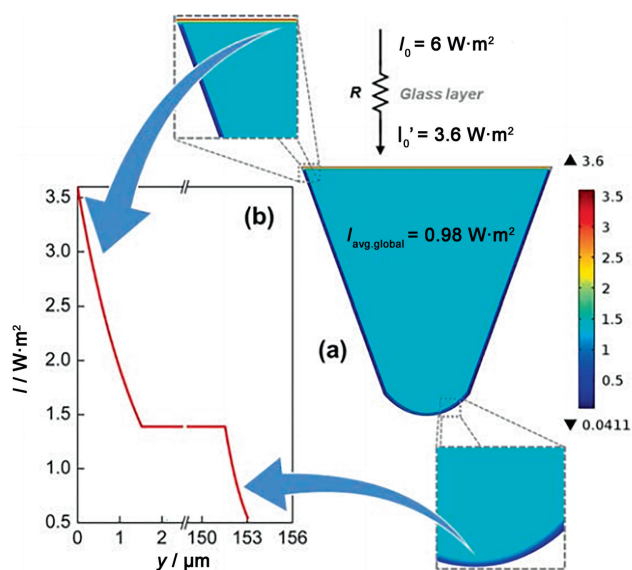


**Fig. 14.** Computational simulation of light distribution at the photocatalyst layers. Adapted with permission of John Wiley.

the residual water on the catalyst surface. Meanwhile, the oxygen performed better than air or nitrogen because oxygen could interact with photocatalyst ( $\text{TiO}_2$ ) and generate radicals to promote the degradation of pollutant.

In addition to  $\text{TiO}_2$  nanoparticles, homogeneous photocatalysts are also widely used in reaction processes such as photocatalytic oxidation [68] and photocatalytic isomerization [74]. Su *et al.* [68] used Eosin Y as a photocatalyst to catalyze the oxygen oxidation of thiophenol to phenyl disulfide within gas–liquid Taylor flow

**Table 5**  
Characteristic times and related dimensionless numbers

Name	Symbol	Definition	Value at $Q = 15\text{--}330 \mu\text{l}\cdot\text{min}^{-1}$
Residence time	$t_R$	$V_R/Q$	840–40 s
Diffusion time in the fluid	$t_D$	$h^2/D$	30 s
Effective diffusion time in catalyst pores	$t_{De}$	$h_p^2/De$	0.007 s
Reaction time	$t_k$	$1/k_{\text{app}}$	60 s
Péclet number	$Pe$	$t_D/t_R$	0.04–0.8
Damköhler I number	$Da_I$	$t_R/t_k$	14–0.7
Damköhler II number	$Da_{II}$	$t_D/t_k$	0.5
Thiele modulus	$\phi$	$(t_{De}/t_k)^{0.5}$	0.01

in a compact photo-microreactor. The reaction process and set-up configuration are shown in Fig. 17. The mass transfer of oxygen from gas phase to liquid phase was enhanced ( $Ha = 0.06$ ) by increasing volumetric flow rate, in this way, the intrinsic kinetics was obtained under kinetic control condition. By fitting the kinetic model to experimental data, the reaction orders of thiophenol and oxygen were measured to be 1 and 2, respectively. Thus, the kinetic equation can be written as Eq. (14). The parameter  $k$  represents the apparent reaction rate constant, including the light intensity and photocatalyst concentration. The experiments under different photon fluxes and photocatalyst loadings were conducted to demonstrate their effects on the reaction rate constant, and the apparent law could be expressed as Eq. (15) (the ranges of photon flux  $q = 0.29\text{--}1.18 \text{ mmol}\cdot\text{s}^{-1}$ , catalyst loading  $\varphi = 0.25\%\text{--}2\%$ ).

$$r = -\frac{dC_{\text{sub}}}{dt} = k C_{\text{sub}} C_{\text{O}_2}^2 \quad (14)$$

$$k = k_0 q^{0.56} \varphi^{0.21} \quad (15)$$

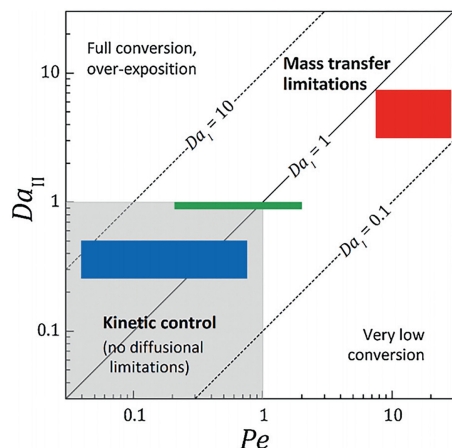


**Fig. 15.** Damköhler II - Peclet diagram showing the relative predominance of each mass transport phenomenon in the reaction cell. The colored rectangles represent the operation range of different photocatalytic microreactors: red and green represents other works, blue represents this work. Adapted with permission of Elsevier.

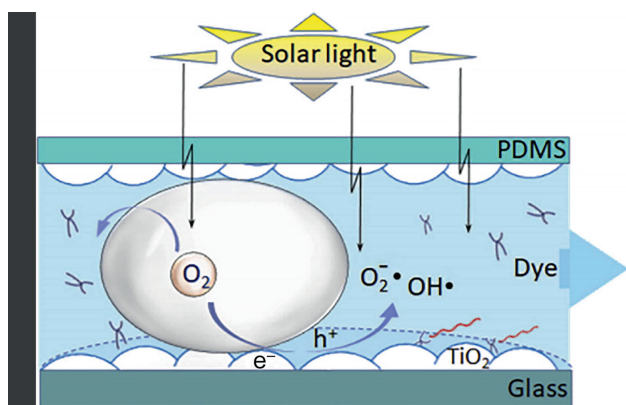


**Fig. 16.** Mechanism of the photocatalytic reaction enhanced by gas phase. Adapted with permission of Elsevier.

Using the similar configuration method of photo-microreactor, Shen *et al.* [10] studied the isomerization of norbornadiene to quadricyclane with the use of triplet photosensitizers. Considering the photon loss due to the absorption and reflection on the microreactor, the accurate intrinsic kinetics was established with the integration of photon flux (the results are shown in Table 4 (Entry 5)). Also in Dr. Su's research group, the photooxidation of benzene to phenol was studied in a continuous-flow microreactor wrapped by blue-LEDs strip [71]. The plug flow model was proved to be available according to the fact that the dimensionless parameter,  $Bo = uL/D$ , was higher than 100. By fitting the experimental values of benzene concentration to the kinetic model, the kinetic results were obtained and listed in Table 4 (Entry 6). The determined kinetic equation was consistent with the outcome inferred by the photooxidation mechanism.

Triplet photosensitizers are commonly used as homogeneous photosensitizers, its activation mechanism is shown in Fig. 18(a). In order to make the photosensitizer easy to be separated from the reaction system, Achi *et al.* [74] developed an ionic liquid moiety photosensitizer, which is a derivative of 4,4'-dimethoxybenzene functionalized with imidazolium arms (as shown in Fig. 18(b)). By utilizing this novel photocatalytic system, the starting and transformed sensitizer could be simply removed by washing the reaction medium with hexane.

### 3.5. Polymerization

Organic polymer materials have replaced metals as the second largest material. The research on the polymerization process has a long history, and in recent years, there are many examples of using microreactors to synthesize polymer materials [75]. However, there are relatively few studies on the polymerization kinetics.

Typically, polymerization is a kind of fast and highly exothermic reactions, which is more obvious for the free radical polymerization [78]. The viscosity of the polymerization reaction system gradually increases as the monomer conversion becomes higher, which will significantly inhibit the mass and heat transfer processes. High temperature condition is beneficial for reducing the viscosity and preventing the polymer products from gelation, however, it can cause the rapid volatilization of solvents with low boiling points [77]. In addition, some polymerization processes also require stringent operation conditions, such as anhydrous and oxygen-free, to ensure a higher molecular weight [1]. Considering the above characteristics, it could be a more efficient way to measure intrinsic kinetics of polymerization via microfluidic technology. The typically polymerization systems (or unit reaction between monomers) and their kinetic regularities that are determined in microreactors are listed in Table 6.

The unit reaction between monomers is the fundamental step of polymerization. Therefore, the kinetic study can start from the unit reaction. Wang *et al.* [15] studied the kinetics of the reaction between aniline and benzoyl chloride, which represents a fundamental chemical step between aromatic amines and aromatic acid chlorides in the polymerization process of poly(*p*-phenylene terephthalamide) (PPTA). The microreactor platform constitutes a micromixer and capillary delay loop. The ideal mixing of the homogeneous reaction system was achieved by increasing the total volumetric flow rate to  $20 \text{ ml}\cdot\text{min}^{-1}$ , and the residence time was precisely controlled by changing the length of the delay loops. The reaction pathways in shown in Fig. 19. Hydrogen chloride, which is the side-product of the main reaction, can further interact with the reactant aniline, constituting a reversible side reaction. It was demonstrated that the main reaction ( $k_1$ ) and forward direction of the side reaction ( $k_2$ ) (completed within a few seconds) are much faster than reverse direction of the side reaction ( $k_{-2}$ ) (completed within 10 min). Therefore, the kinetic experiments were performed in different ranges of time and temperature to determine different kinetic parameters. Table 6 (Entry 1) shows the obtained results, which guided the design of microreactor and operation conditions in the polymerization of *p*-phenylenediamine with terephthaloyl chloride [79].

The reaction of phenyl isocyanate with monoalcohol is of great importance to prepare carbamates and polyurethane type polymers. López *et al.* [76] studied its kinetic regularities with different kinds of alcohols (primary or secondary) in a glass microchannel reactor. The pseudo-first-order kinetic model was used to analyze the reaction rate constants, and the experimental results (shown in Table 6, Entry 2) indicated that the reaction with primary alcohols has higher reaction rate constant due to the less steric hindrance.

Free radical polymerization usually has a high reaction enthalpy and ultra-fast chain propagation rate. Therefore, the characteristics of microreactors, with respect to the rapid heat transfer and precise control of residence time seem particularly important for kinetic measurement of free radical polymerization. Qiu *et al.* [77] developed a microreactor platform to study the kinetics of acrylic acid polymerization in aqueous solution using potassium persulfate as initiator. Capillary tubes with different lengths were assembled by multi-port valves, realizing the free switching of 14 different tube volumes (from 6.6 ml to 123.1 ml) in one micro device (shown in Fig. 20). In order to accelerate the reaction and



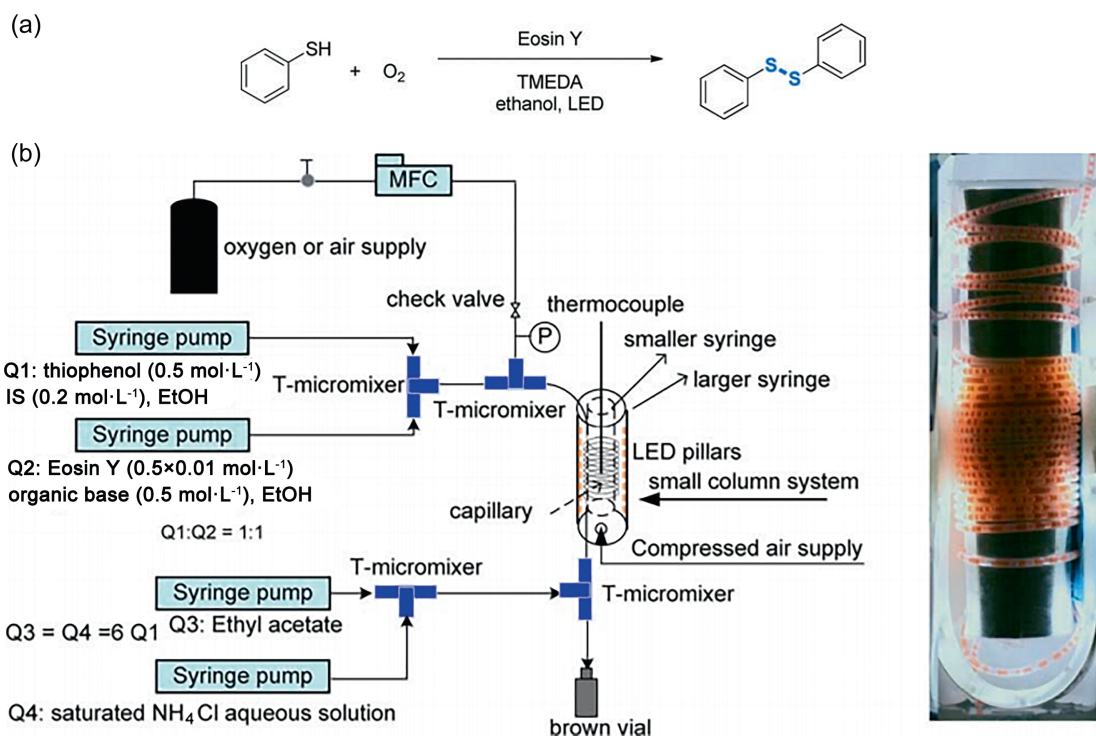
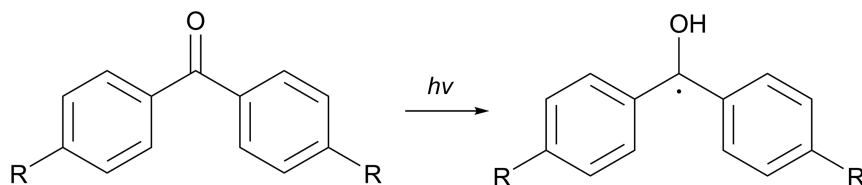


Fig. 17. (a) Schematic of the photocatalytic oxidation of thiophenol. (b) Set-up configuration and a picture of an opening photochemical column system. Adapted with permission of John Wiley.

### (a) Mechanism of triplet photosensitizer activated by radiation



### (b) Structure of ionic liquid moiety photosensitizer

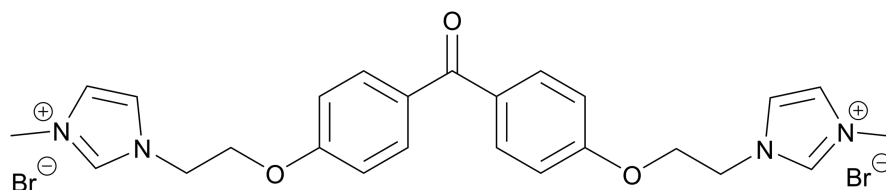


Fig. 18. The schematic of (a) photosensitizer activation mechanism and (b) the structure of an ionic liquid photosensitizer.

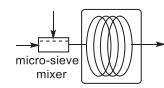
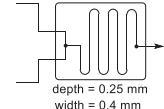
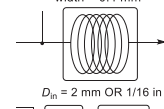
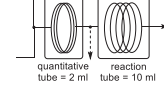
obtain the kinetic regularities at high monomers conversion rate, the kinetic experiments were carried out under high temperature ranges from 80 to 95 °C. No evaporation of water was observed due to the absence of gas space in capillary tubes. The obtained kinetic model is shown in Eq. (16). Actually, the order of acrylic acid was measured to be 1.41, which basically conforms to the theoretical result 1.5. The fact that the order of monomer is higher than 1 is caused by the secondary monomer-enhanced decomposition of the initiator [80].

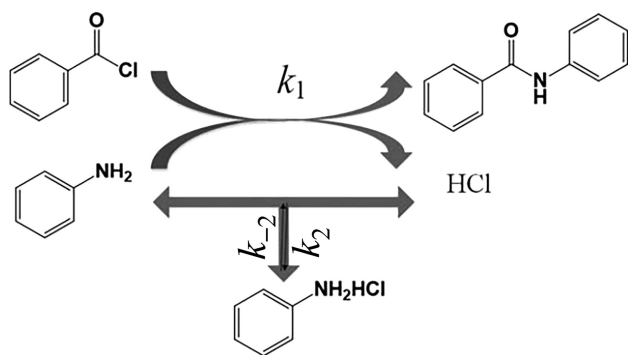
$$r = -\frac{dC_{AA}}{dt} = 8.0 \times 10^8 \exp\left(-\frac{6.74 \times 10^4}{RT}\right) C_{AA}^{1.5} C_{KBS}^{0.5} \quad (16)$$

Another example of free radical polymerization is the synthesis of branched poly(butyl acrylate) via the solution polymerization of butyl acrylate and divinylbenzene, which was studied by Xiang *et al.* [78] in a capillary microreactor. The polymerization process was initiated with 2,2'-azobisisobutyronitrile and mediated with chain transfer agent dodecanethiol to regulate the branching degree. The comparison between the microreactor and the batch reactor was presented from various aspects, including the reaction rate at different reaction stages, temperature profiles and polymer product qualities. It was demonstrated that the polymerization was initiated quickly in the microreactor because the generated free radicals would rapidly contact with monomers and propagate

**Table 6**

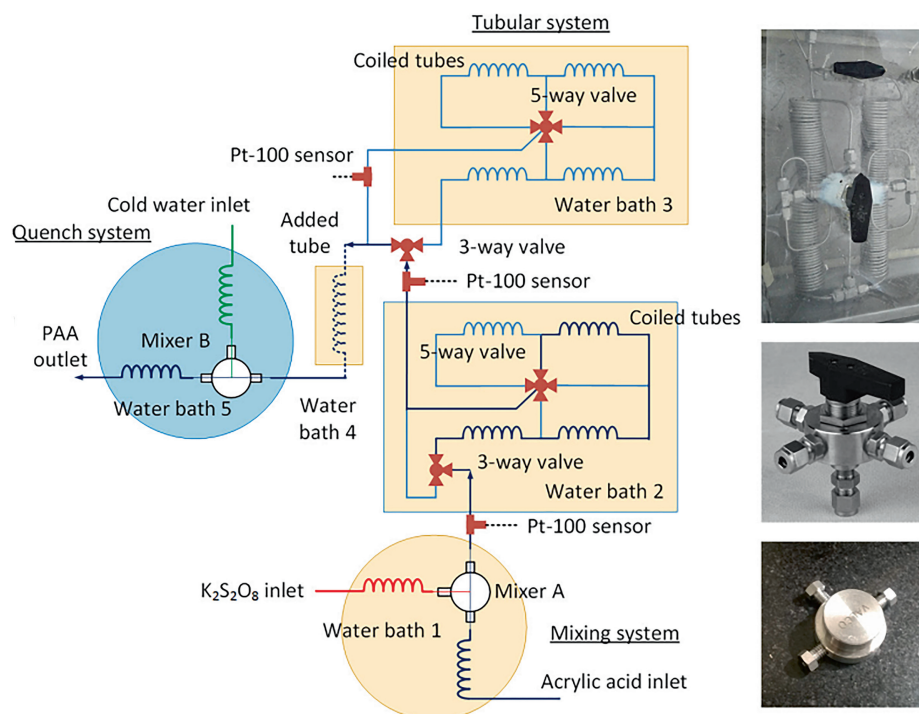
An overview of some the typical studies on polymerization kinetics

Entry	Authors	Reactants	Catalyst (initiator)	Phase state	Kinetic equation	Activation energy / $\text{kJ}\cdot\text{mol}^{-1}$	Microreactor scheme
1	Wang, et al., 2015 [15]	Aniline, benzoyl chloride	/	Homogeneous	$\frac{dC_{Al}}{dt} = -k_1 C_{Al} C_{BC} - k_2 C_{Al} C_{HCl} + k_{-2} C_{Al} C_{HCl}$	8.14 ( $k_1$ ) 8.14 ( $k_2$ ) 4.14 ( $k_{-2}$ )	
2	López, et al., 2019 [76]	Phenyl isocyanate, monoalcohol	/	Homogeneous	$r = k C_{PhNCO}$	30.4 (propan-1-ol) 38.1 (propan-2-ol)	
3	Qiu, et al., 2016 [77]	Acrylic acid	Potassium persulfate	Homogeneous	$r = k C_{AA}^{1.5} C_{KBS}^{0.5}$	67.4	
4	Lu and Wang, 2019 [1]	$\delta$ -valerolactone	TBD BnOH	Homogeneous	$r = k C_{\delta-VL} C_{TBD}^0$	7.30	

**Fig. 19.** Reaction pathways of aniline with benzoyl chloride. Adapted with permission of John Wiley.

in the narrow-confined channel. The reaction rate in batch reactor was higher in the middle and late stages because the released heat was accumulated in the reactor and the reaction was accelerated by the uncontrollable temperature. As a result, the molecular weight dispersity ( $D$ ) of the final product was 3.4 in the batch operation, much larger than that of 2.1 in the microreactor. Besides, due to the large mass transfer coefficient and reduced diffusion pathway, the polymer with higher branching degrees was synthesized in the microreactor.

The last example is the kinetic study of  $\delta$ -valerolactone ( $\delta$ -VL) ring-opening polymerization (ROP) to prepare aliphatic polyester in a gas-driven droplet flow microreactor [1]. The cyclic ester ROP using 1,5,7-triazabicycl[4.4.0]dec-5-ene (TBD) as catalyst and benzyl alcohol (BnOH) as initiator is shown in Fig. 21(a). This reaction requires all starting materials to be strictly dehydrated. In order to further reduce the chemical consumption, a novel

**Fig. 20.** Schematic of the microreactor platform and pictures of the main elements. Adapted with permission of Elsevier.

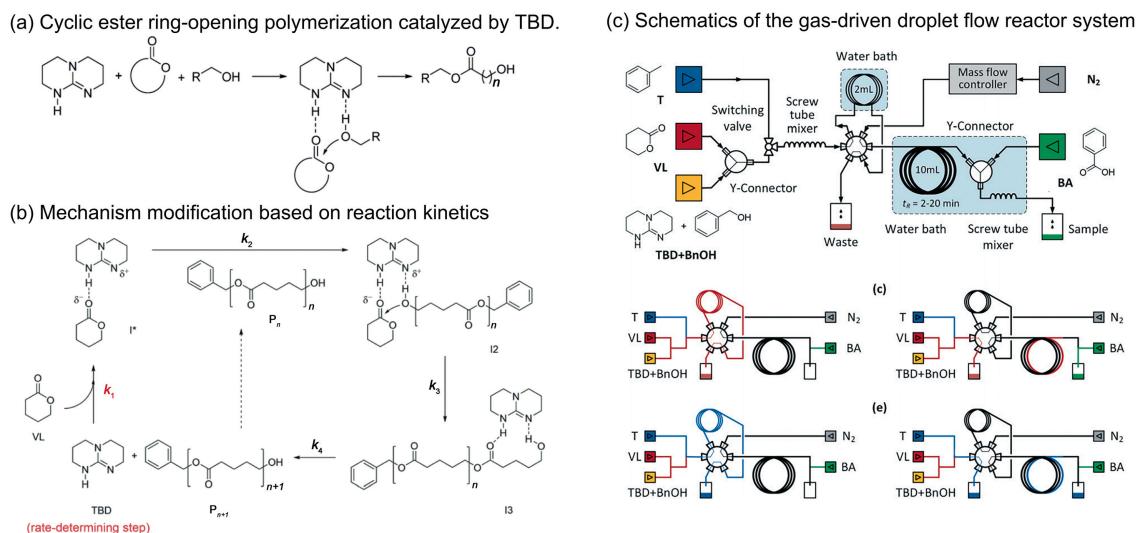


**Fig. 21.** (a) The cyclic ester ring-opening polymerization and (b) its catalytic mechanism deduced from the obtained kinetic regularities. (c) Set-up configuration of microreactor platform for kinetic measurement. Adapted with permission of Royal Society of Chemistry.

microreactor platform was established as shown in Fig. 21(c), in which only 2 ml solution was used for each test. The kinetic experiments were performed under different initial concentrations of TBD and BnOH to determine their reaction orders respectively. And it was demonstrated that the reaction order of monomers  $\delta$ -VL and catalyst TBD are both 1, but the concentration of initiator BnOH had little effect on the reaction rate. Based on the obtained kinetic regularities, the modified mechanism was put forward (Fig. 21 (b)), which implied that the monomer activation was the rate-determining step and TBD would leave the hydroxyl group in each catalytic round.

### 3.6. Other reactions

In this section, the chemical reactions that are not included in the above five categories will be covered, including rearrangement [81,82], alkylation [83], hydration [4], decomposition [2,84] and so on. Although the kinetic laws of these reactions have completely different characteristics, the microfluidic technology plays an important role in their determination processes.

The homogeneous reaction kinetics is introduced first. Zhang *et al.* [85] studied the dehydrochlorination of dichloropropanol (DCP) with caustic soda solution in a capillary microreactor. Compared with the reported kinetic regularities measured in batch operation, the more accurate results were obtained in the microreactor due to the efficient mixing and the precise control of reaction time (less than 1 min) for this fast reaction. The kinetic model of second-order with respect to DCP concentration was demonstrated to be more suitable to fit the experimental data, rather than the first-order model proposed in the previous reports. The concrete kinetic model and measured activation energy are exhibited in Table 7 (Entry 1).

Hofmann rearrangement is a strongly exothermic reaction that are conducted to convert a primary amide to a primary amine in organic synthesis. Usually, extremely low temperature ( $-5$  to  $5$  °C) is required in batch reactor to prevent local overheating by reducing reaction rate. Huang *et al.* [81] studied the kinetic characteristics of Hofmann rearrangement of 1,1-cyclohexanediamic acid monoamide to prepare Gabapentin (Table 7, Entry 2). Based on the enhancement of heat transfer in a microreaction system, the pseudo-isothermic condition could be obtained even at relatively high temperature. In this way, the kinetic regularities in

the temperature range from 30 to 45 °C were obtained, which was essential for the process intensification in the microreaction process to prepare Gabapentin.

Another example of rearrangement reaction is the Beckmann rearrangement of cyclohexanone oxime to prepare  $\epsilon$ -caprolactam (Table 7, Entry 3) [82]. The kinetic measurement using trifluoroacetic acid (TFA)/acetonitrile as the catalytic system is hard to perform in batch reactor because of the extremely fast reaction rate and evaporation of TFA under high temperature. The reaction mechanism of Beckmann rearrangement is shown in Fig. 22, which is constituted by a series of elementary reactions. The kinetic equations should be established based on all of these transformations that comply with the law of mass action (Eqs. (17)–(21)), and the kinetic parameters in each step could be fitted together according to the curves of concentrations versus time in a set of kinetic experiments (as shown in Fig. 23). A large amount of experimental data is often required to ensure the fitting accuracy of multiple parameters. Analyzing the relative reaction rates in each step, the esterification and transposition reactions of the intermediate were both supposed to be the rate-determining steps.

$$\frac{dC_{\text{COX}}}{dt} = -k_1 C_{\text{COX}} C_{\text{TFA}} + k_{-1} C_{\text{COXTFA}} C_{\text{H}_2\text{O}} \quad (17)$$

$$\frac{dC_{\text{TFA}}}{dt} = -k_1 C_{\text{COX}} C_{\text{TFA}} + k_{-1} C_{\text{COXTFA}} C_{\text{H}_2\text{O}} + k_2 C_{\text{COXTFA}} C_{\text{H}_2\text{O}} \quad (18)$$

$$\frac{dC_{\text{COXTFA}}}{dt} = k_1 C_{\text{COX}} C_{\text{TFA}} - k_{-1} C_{\text{COXTFA}} C_{\text{H}_2\text{O}} - k_2 C_{\text{COXTFA}} C_{\text{H}_2\text{O}} \quad (19)$$

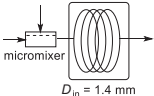
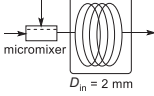
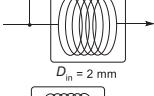
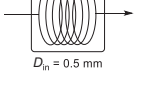
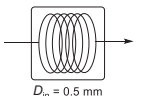
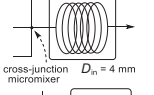
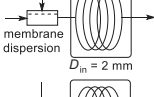
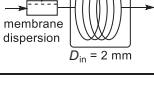
$$\frac{dC_{\text{H}_2\text{O}}}{dt} = \frac{dC_{\text{COXTFA}}}{dt} \quad (20)$$

$$\frac{dC_{\text{CPL}}}{dt} = k_2 C_{\text{COXTFA}} C_{\text{H}_2\text{O}} \quad (21)$$

Similar kinetic modeling method was used to study the thermal dissociation and oligomerization of dicyclopentadiene in a capillary microreactor (Table 7, Entry 4). The use of microreactor significantly improved the safety of this process under high temperature (180 to 240 °C) and high pressure (5 MPa) due to the rapid heat-removal ability and trace consumption of reactants. Cyclopentadiene was the targeted intermediate product formed *via* the thermal

Table 7

An overview of some kinetic studies on other kinds of reactions

Entry	Authors	Reactants	Catalyst (initiator)	Phase state	Kinetic equation	Activation energy / $\text{kJ}\cdot\text{mol}^{-1}$	Microreactor scheme
1	Zhang, et al., 2012 [85]	2,3-DCP, NaOH	/	Homogeneous	$r = kC_{2,3\text{-DCP}}^2 C_{\text{OH}^-}$	150	
2	Huang, et al., 2017 [81]	CAM, NaClO, NaOH	/	Homogeneous	$r = kC_{\text{CAM}}^{0.9} C_{\text{NaClO}}^{0.85} C_{\text{NaOH}}^{0.34}$	99.5	
3	Du, et al., 2018 [82]	Cyclohexanone oxime	TFA/CH <sub>3</sub> CN	Homogeneous	$\frac{dC_{\text{TFA}}}{dt} = -k_1 C_{\text{COX}} C_{\text{TFA}} + k_{-1} C_{\text{COXTFA}} C_{\text{H}_2\text{O}} + k_2 C_{\text{COXTFA}} C_{\text{H}_2\text{O}}$	93 ( $k_1$ ) 128 ( $k_{-1}$ ) 152 ( $k_2$ ) (TFA/CH <sub>3</sub> CN = 2:1)	
4	Yao, et al., 2020 [2]	Dicyclopentadiene	/	Homogeneous	$\frac{dC_{\text{CPD}}}{dt} = 2k_1 C_{\text{endo}} + 2k_{-2} C_{\text{exo}} - 2k_{-1} C_{\text{CPD}}^2 - k_3 C_{\text{CPD}} C_{\text{endo}} - k_4 C_{\text{CPD}} C_{\text{exo}} - 2k_2 C_{\text{CPD}}^2$	131 ( $k_1$ ) 62.0 ( $k_{-1}$ ) 69.0 ( $k_2$ ) 157 ( $k_{-2}$ ) 101 ( $k_3$ ) 104 ( $k_4$ )	
5	Lin, et al., 2020 [3]	PVA, n-butanol	HCl	Homogeneous	$-\frac{dC_d}{dt} = k_{2m} C_{A,0} C_{H^+,0} C_d$	36.4	
6	Li, et al., 2019 [83]	Isobutane, 2-butene	Sulfuric acid	Liquid-liquid	$\frac{d[\text{TMP}]}{dt} = k_1 [C_4^-] [iC_4]$ $\frac{d[\text{DMH}]}{dt} = k_2 [C_4^-] [iC_4]$ $\frac{d[\text{HE}]}{dt} = k_3 [C_4^-]^2 [iC_4]$ $\frac{d[\text{DMH}]}{dt} = 2k_2 [C_4^-]^2 [iC_4]$	64.7 ( $k_1$ ) 85.6 ( $k_2$ ) 132 ( $k_3$ ) 105 ( $k_4$ )	
7	Guo, et al., 2020 [4]	Acrylonitrile	Free cells containing NHase	Liquid-liquid	$r = \frac{r_{\text{max}} C_s}{K_m + K_h C_s + K_p C_p}$	/	 

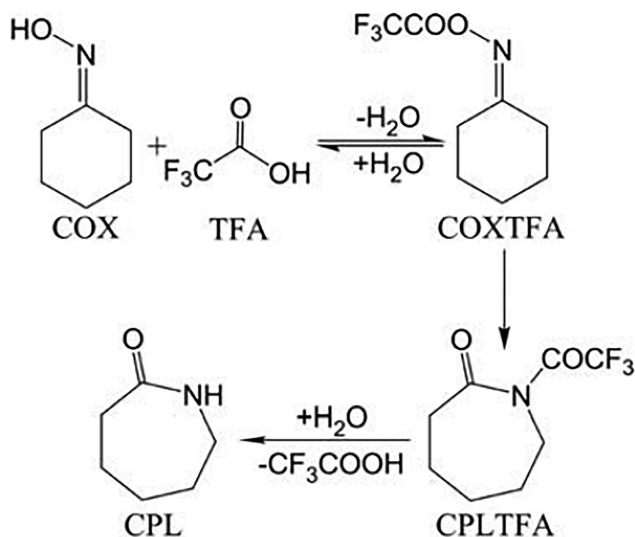


Fig. 22. Mechanism of Beckmann rearrangement of cyclohexanone oxime catalyzed by TFA/acetonitrile. Adapted with permission of John Wiley.

dissociation of dicyclopentadiene, and the cascade oligomerization was the undesired side reaction. Based on the deep understanding of the kinetic differences between thermal dissociation and oligomerization, the yield of cyclopentadiene was improved by reasonable design of residence time and temperature.

Lin et al. [3] studied the kinetic characteristics of the acetal reaction between polyvinyl alcohol (PVA) and *n*-butanal catalyzed by

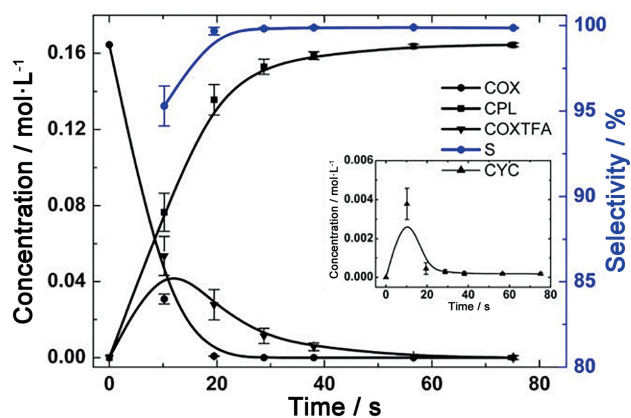


Fig. 23. A typical concentration profiles of different products in Beckmann rearrangement of cyclohexanone oxime. Adapted with permission of John Wiley.

hydrogen chloride in aqueous solution. A cross-junction micromixer was used to enhance the mixing ability, and multiple capillary delay loops with different lengths were connected by a 7-way valve to realize precise control of different residence times. The reported reaction mechanism indicated that the acetal reaction was composed of multiple reaction steps [86] which could be decoupled by applying different reaction conditions. In this way, the reaction rate constants of the hemiacetal reaction and intramolecular acetal reaction were determined respectively, and the obtained kinetic results are listed in Table 7 (Entry 5).

Two examples of measuring heterogeneous reaction kinetics in microreactors are introduced below. The sulfuric acid alkylation is a typical liquid–liquid heterogeneous reaction. The catalyst, sulfuric acid, is in aqueous phase and the reactant, mixed liquefied gas of isobutane/2-butene, is in organic phase. Li *et al.* [83] demonstrated that the kinetic model determined in batch reactors cannot predict the experimental results obtained in the microreactor at all, which was caused by the effect of mass transfer on the reaction rate. The droplet diameter obtained in the microreactor was about 50  $\mu\text{m}$  under the applied conditions for kinetic measurement.

However, the typical droplet size in stirring tank is 1–2 mm. Combining with the kinetics results obtained in microreactor (Table 7, Entry 6), the computational fluid dynamics indicated that when the droplet diameter was set as 50  $\mu\text{m}$ , mass transfer didn't affect the reaction rate at all (Fig. 24 (a-1), (a-2) and (a-3)), however, the effect becomes significant by increasing the diameter to 1.5 mm (Fig. 24 (b-1), (b-2) and (b-3)).

The last example is about the kinetic study on a liquid–liquid biocatalytic reaction. The hydration of acrylonitrile to acrylamide catalyzed by free cells containing nitrile hydratase was studied in

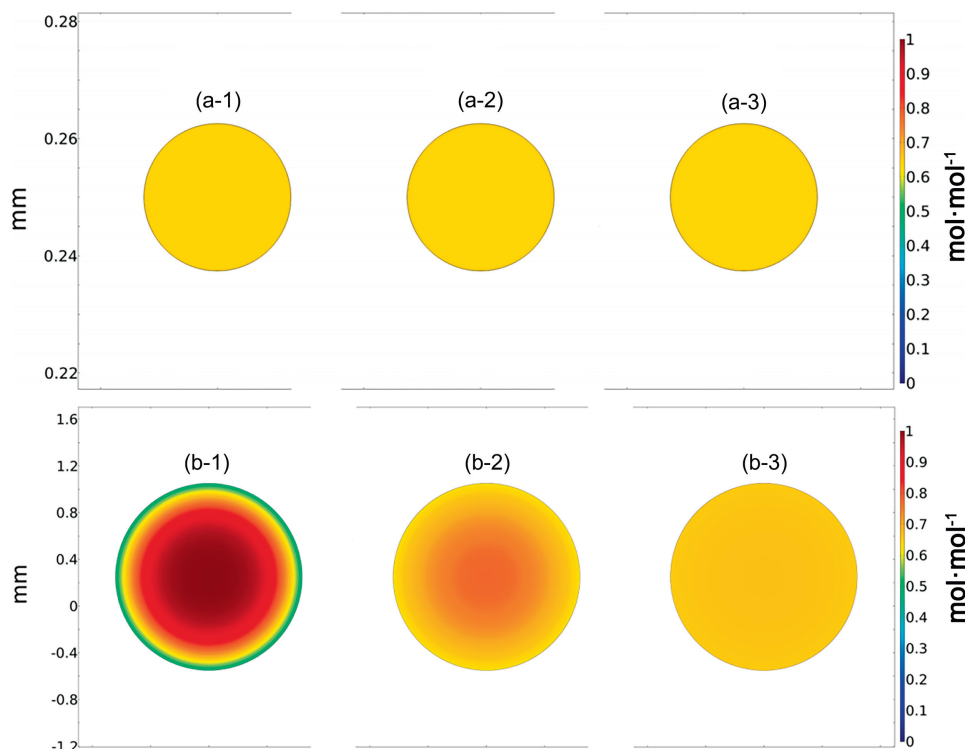


**Fig. 24.** Butene content calculated using COMSOL software at different diffusion coefficients. Conditions of the three experiments above:  $T = 0\text{ }^{\circ}\text{C}$ ,  $d = 50\text{ }\mu\text{m}$  (a-1)  $D = 2.4 \times 10^{-8}\text{ m}^2\cdot\text{s}^{-1}$  (a-2)  $D = 2.4 \times 10^{-5}\text{ m}^2\cdot\text{s}^{-1}$ ; (a-3)  $D = 2.4 \times 10^{-2}\text{ m}^2\cdot\text{s}^{-1}$ . Conditions of the three experiments below:  $T = 0\text{ }^{\circ}\text{C}$ ,  $d = 2.5\text{ mm}$  (b-1)  $D = 2.4 \times 10^{-8}\text{ m}^2\cdot\text{s}^{-1}$  (b-2)  $D = 2.4 \times 10^{-7}\text{ m}^2\cdot\text{s}^{-1}$ ; (b-3)  $D = 2.4 \times 10^{-6}\text{ m}^2\cdot\text{s}^{-1}$ . Adapted with permission of American Chemical Society.

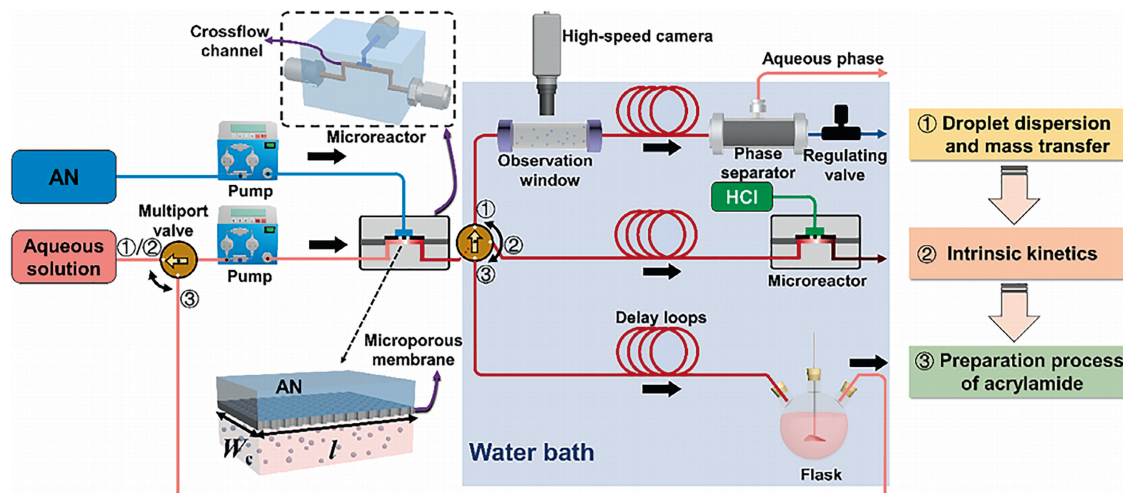


**Fig. 25.** Schematic overview of the microstructured chemical system for biohydration of acrylonitrile. Adapted with permission of John Wiley.

a microstructured chemical system [4]. This highly integrated microreaction system combined three important functions, which included the determination of droplet dispersion and mass transfer, measurement of intrinsic kinetics and preparation of acrylamide product (see Fig. 25). The interphase mass transfer rate was enhanced by adjusting the microstructure size and flow conditions. As a result, the acrylonitrile droplets with an average diameter of 40  $\mu\text{m}$  and the volumetric mass transfer coefficient of  $0.33 \text{ s}^{-1}$  were obtained. Under this condition, the biohydration was totally controlled by intrinsic kinetics because the calculated Damköhler number ( $Da = \frac{r}{k_{L,a} \Delta C_M}$ ) was smaller than 0.1. The intrinsic kinetics model (Table 7, Entry 7) incorporating the effects of product inhibition and cell inactivation was determination and used to guide the design of recirculation microchemical system for the preparation of acrylamide product.

#### 4. Summary and Outlook

This review comprehensively summarizes the recent research progresses on the reaction kinetics that are determined in microreactors, whose advantages are fully exhibited in different reaction categories. For nitration reaction, the rapid heat transfer and precise control of reaction time in a few seconds provide convenience for kinetic measurements in these fast and highly exothermic reactions. For oxidation reaction, the safety issue is always regarded to be the first element especially when using the pure oxygen as oxidant. Microfluidic technology can minimize the risk by reducing the reactant consumption as low as possible and exerting limit to the explosion propagation in confined space. For hydrogenation reaction in the presence of solid catalysts, the determination of intrinsic kinetics must be based on the enhanced mass transfer performances including both the external and internal diffusion, which is easier to be achieved in the microreactor system because of its higher mass transfer coefficient and larger surface-to-volume ratio. For photochemical reaction, the uniform light-intensity distribution, which is the prerequisite for accurate measurement of kinetics, can be easily realized in microchannels due to the short light penetration depth. For polymerization reaction, the efficient mixing and excellent mass and heat transfer performances in microreaction system are badly required to guarantee the uniform conditions when the viscosity of the reaction system gets higher and higher as the monomer conversion increases. Except for these typical reactions, microfluidic technology has also been successfully used to solve different kinds of dilemmas in the kinetic measurement of some specific reactions, such as the extremely fast and exothermic rearrangement reaction, and acetal reaction under the conditions of large mixing ratio and viscosity.

This work also provides an overview of the state-of-the-art innovations of micro-platforms, which were dedicatedly configured to meet the requirement for rapid and efficient measurement of reaction kinetics, specifically including (1) inline collection and analysis of experimental data and (2) multiple kinetic results obtained in one set of experiment. Throughout all of the excellent studies covered in this work, there are still some vital issues that require to be further explored.

First, most of the descriptions about the excellent performances of microreactors are qualitative, which is in sharp contrast with the precise and quantitative kinetic results obtained in them. Thus, it is very meaningful to put more effort to quantify the performances of the established microreactor system, with respect to its mixing time, mass and heat transfer coefficient and residence time distribution.

Second, most of studies are based on microfluidic technology to solve a critical problem in the kinetic measurement of a certain reaction system. However, the research on the same reaction in

different microreactors is neglected. Microreactors with diversified internal structures and distinct feature sizes have different mixing and mass transfer characteristics, which may lead to entirely different kinetic regularities. Based on the deep understanding towards the effect of microstructure on the reaction kinetics, it is expected to establish a set of two-way judgement criteria to answer not only what kind of reaction is suitable to be carried out in a microreactor, but also what kind of microreactor is best for the reaction.

Third, most of the kinetic studies in microreactors still focus on the conventional reactions with relatively clear mechanism and straightforward pathways. The kinetic determination for the complex reactions still relies on decoupling multiple pathways by adjusting reaction conditions, which can greatly increase the workload. Moreover, the kinetic modeling method is usually simplified according to equilibrium hypothesis and steady-state hypothesis, in which the terms of reaction intermediate concentrations are removed, and the obtained kinetic regularities cannot reflect the reaction mechanism anymore. Based on the development of inline analysis and its combination with microfluidic technology, it is promising to obtain more information on reaction transition states and intermediates, so as to pry into the essential interaction laws of matters.

Fourth, the equipment innovation is particularly critical to the development of microfluidic technology, and this progress definitely involves the intersection and integration of multiple disciplines. Combining the technologies of chemical engineering, mechanical engineering, automation and computer, it is promising to develop a highly integrated and intelligent micro-platform for continuous tests of reaction kinetics.

In conclusion, the study of reaction kinetics in microreactors is of great significance because it is helpful to understand the interface effect, mass transfer regularities and reaction mechanism at micro-nano scale, which may not comply with the classical theories that are established in the macroscopic dimension. Through unceasing efforts devoted to understand the interaction laws between matters in a confined space, the innovative research method and new theory may be established in microreactors, which could be a milestone in the development of microfluidic technology.

#### Declaration of Competing Interest

The authors declare that they have no known competing financial interests or personal relationships that could have appeared to influence the work reported in this paper.

#### Acknowledgements

We gratefully acknowledge financial support from National Natural Science Foundation of China (21991104).

#### Supplementary Material

Supplementary data to this article can be found online at <https://doi.org/10.1016/j.cjche.2021.08.023>.

#### References

- [1] S. Lu, K. Wang, Kinetic study of TBD catalyzed  $\delta$ -valerolactone polymerization using a gas-driven droplet flow reactor, *React. Chem. Eng.* 4 (2019) 1189–1194.
- [2] Z. Yao, X. Xu, Y. Dong, X. Liu, B. Yuan, K. Wang, K. Cao, G. Luo, Kinetics on thermal dissociation and oligomerization of dicyclopentadiene in a high temperature & pressure microreactor, *Chem. Eng. Sci.* 228 (2020) 115892.
- [3] X. Lin, K. Wang, B. Zhou, G. Luo, A microreactor-based research for the kinetics of polyvinyl butyral (PVB) synthesis reaction, *Chem. Eng. J.* 383 (2020) 123181.

- [4] M. Guo, Q. Chen, Y. Liang, Y. Wang, G. Luo, H. Yu, Experimental and model-based study of biohydration of acrylonitrile to acrylamide in a microstructured chemical system, *AIChE J.* 66 (2020) e16298.
- [5] A. Hommes, A.J. ter Horst, M. Koeslag, H.J. Heeres, J. Yue, Experimental and modeling studies on the Ru/C catalyzed levulinic acid hydrogenation to  $\gamma$ -valerolactone in packed bed microreactors, *Chem. Eng. J.* 399 (2020) 125750.
- [6] Z. Yan, Z. Ma, J. Deng, G. Luo, Mechanism and kinetics of epoxide ring-opening with carboxylic acids catalyzed by the corresponding carboxylates, *Chem. Eng. Sci.* 242 (2021) 116746.
- [7] Z. Yan, J. Tian, K. Wang, K.D.P. Nigam, G. Luo, Microreaction processes for synthesis and utilization of epoxides: A review, *Chem. Eng. Sci.* 229 (2021) 116071.
- [8] J. Deng, J. Zhang, K. Wang, G. Luo, Microreaction Technology for Synthetic Chemistry, *Chinese J. Chem.* 37 (2019) 161–170.
- [9] Y. Lu, D. Xin, J. Zhang, G. Luo, Modeling ethyl diazoacetate synthesis in an adiabatic microchemical system, *Chem. Eng. J.* 273 (2015) 406–412.
- [10] C. Shen, M. Shang, H. Zhang, Y. Su, A UV-LEDs based photomicroreactor for mechanistic insights and kinetic studies in the norbornadiene photoisomerization, *AIChE J.* 66 (2020) e16841.
- [11] H. Keles, F. Susanne, H. Livingstone, S. Hunter, C. Wade, R. Bourdon, A. Rutter, Development of a robust and reusable microreactor employing laser based mid-IR chemical imaging for the automated quantification of reaction kinetics, *Org. Process Res. Dev.* 21 (2017) 1761–1768.
- [12] D. Russo, G. Tomaiuolo, R. Andreozzi, S. Guido, A.A. Lapkin, I. Di Somma, Heterogeneous benzaldehyde nitration in batch and continuous flow microreactor, *Chem. Eng. J.* 377 (2019) 120346.
- [13] M.N. Kashid, A. Renken, L. Kiwi-Minsker, Gas–liquid and liquid–liquid mass transfer in microstructured reactors, *Chem. Eng. Sci.* 66 (2011) 3876–3897.
- [14] Z. Wen, M. Yang, S. Zhao, F. Zhou, G. Chen, Kinetics study of heterogeneous continuous-flow nitration of trifluoromethoxybenzene, *React. Chem. Eng.* 3 (2018) 379–387.
- [15] P. Wang, K. Wang, J. Zhang, G. Luo, Kinetic study of reactions of aniline and benzoyl chloride in a microstructured chemical system, *AIChE J.* 61 (2015) 3804–3811.
- [16] N. Padoin, L. Andrade, J. Ângelo, A. Mendes, R.D.F.P. Moreira, C. Soares, Intensification of photocatalytic pollutant abatement in microchannel reactor using TiO<sub>2</sub> and TiO<sub>2</sub>-graphene, *AIChE J.* 62 (2016) 2794–2802.
- [17] C. Dong, K. Wang, J.S. Zhang, G.S. Luo, Reaction kinetics of cyclohexanone ammoxidation over TS-1 catalyst in a microreactor, *Chem. Eng. Sci.* 126 (2015) 633–640.
- [18] M. Krivec, A. Pohar, B. Likozar, G. Dražič, Hydrodynamics, mass transfer, and photocatalytic phenol selective oxidation reaction kinetics in a fixed TiO<sub>2</sub> microreactor, *AIChE J.* 61 (2015) 572–581.
- [19] J.P. McMullen, K.F. Jensen, Rapid determination of reaction kinetics with an automated microfluidic system, *Org. Process Res. Dev.* 15 (2011) 398–407.
- [20] N.T. Nguyen, Z.G. Wu, Micromixers - a review, *J. Micromech. Microeng.* 15 (2005) R1–R16.
- [21] K. Wang, G. Luo, Microflow extraction: A review of recent development, *Chem. Eng. Sci.* 169 (2017) 18–33.
- [22] J. Zhang, K. Wang, A.R. Teixeira, K.F. Jensen, G. Luo, Design and scaling up of microchemical systems: a review, *Annu. Rev. Chem. Biomol.* 8 (2017) 285–305.
- [23] J. Sui, J. Yan, D. Liu, K. Wang, G. Luo, Continuous synthesis of nanocrystals via flow chemistry technology, *Small* 16 (2020) 1902828.
- [24] F. Benito-Lopez, W. Verboom, M. Kakuta, J.H.G.E. Gardeniers, R.J.M. Egberink, E. R. Oosterbroek, A. van den Berg, D.N. Reinhoudt, Optical fiber-based on-line UV/Vis spectroscopic monitoring of chemical reaction kinetics under high pressure in a capillary microreactor, *Chemical communications (Cambridge, England)* (2005) 2857–2859.
- [25] A. Muto, M. Ebata, A. Inoue, Development of a microreactor for rapid analysis of chemical reaction kinetics with absorption spectroscopy, *IEEE*, 2008.
- [26] X. Duan, J. Tu, A.R. Teixeira, L. Sang, K.F. Jensen, J. Zhang, An automated flow platform for accurate determination of gas-liquid-solid reaction kinetics, *React. Chem. Eng.* 5 (2020) 1751–1758.
- [27] J.S. Moore, C.D. Smith, K.F. Jensen, Kinetics analysis and automated online screening of aminocarbonylation of aryl halides in flow, *React. Chem. Eng.* 1 (2016) 272–279.
- [28] Y.F. Han, M.J. Kahlich, M. Kinne, R.J. Behm, Kinetic study of selective CO oxidation in H<sub>2</sub>-rich gas on a Ru/ $\gamma$ -Al<sub>2</sub>O<sub>3</sub> catalyst, *Phys. Chem. Chem. Phys.* 4 (2002) 389–397.
- [29] J.S. Moore, K.F. Jensen, “Batch” Kinetics in flow: online IR analysis and continuous control, *Angewandte Chemie International Edition* 53 (2014) 470–473.
- [30] K. Wang, Y.C. Lu, Y. Xia, H.W. Shao, G.S. Luo, Kinetics research on fast exothermic reaction between cyclohexanecarboxylic acid and oleum in microreactor, *Chem. Eng. J.* 169 (2011) 290–298.
- [31] C. Zhang, J. Zhang, G. Luo, Kinetics determination of fast exothermic reactions with infrared thermography in a microreactor, *J. Flow Chem.* 10 (2020) 219–226.
- [32] J.S. Zhang, C.Y. Zhang, G.T. Liu, G.S. Luo, Measuring enthalpy of fast exothermal reaction with infrared thermography in a microreactor, *Chem. Eng. J.* 295 (2016) 384–390.
- [33] Z. Lan, Y. Lu, Continuous nitration of o-dichlorobenzene in micropacked-bed reactor: process design and modelling, *J. Flow Chem.* 11 (2021) 171–179.
- [34] J. Grant, P.T.O. Kane, B.R. Kimmel, M. Mrksich, Using microfluidics and imaging SAMDI-MS to characterize reaction kinetics, *ACS Cent. Sci.* 5 (2019) 486–493.
- [35] E. Fradet, P. Abbyad, M.H. Vos, C.N. Baroud, Parallel measurements of reaction kinetics using ultralow-volumes, *Lab Chip* 13 (2013) 4326–4330.
- [36] C. Zheng, B. Zhao, K. Wang, G. Luo, Determination of kinetics of CO<sub>2</sub> absorption in solutions of 2-amino-2-methyl-1-propanol using a microfluidic technique, *AIChE J.* 61 (2015) 4358–4366.
- [37] A.A. Kulkarni, Continuous flow nitration in miniaturized devices, *Beilstein J. Org. Chem.* 10 (2014) 405–424.
- [38] L. Li, C. Yao, F. Jiao, M. Han, G. Chen, Experimental and kinetic study of the nitration of 2-ethylhexanol in capillary microreactors, *Chem. Eng. Process. Process Intensif.* 117 (2017) 179–185.
- [39] C. Zhang, J. Zhang, G. Luo, Kinetic study and intensification of acetyl guaiacol nitration with nitric acid–acetic acid system in a microreactor, *J. Flow Chem.* 6 (2016) 309–314.
- [40] J. Tan, L. Du, Y.C. Lu, J.H. Xu, G.S. Luo, Development of a gas–liquid microstructured system for oxidation of hydrogenated 2-ethyltetrahydroanthraquinone, *Chem. Eng. J.* 171 (2011) 1406–1414.
- [41] K. Bawornrattanaboonya, N. Laosiripojana, A.S. Mujumdar, S. Devahastin, Catalytic partial oxidation of CH<sub>4</sub> over bimetallic Ni-Re/Al<sub>2</sub>O<sub>3</sub>: Kinetic determination for application in microreactor, *AIChE J.* 64 (2018) 1691–1701.
- [42] R.H. Nibelke, M.A.J. Campman, J.H.B.J. Hoebink, G.B. Marin, Kinetic Study of the CO Oxidation over Pt/ $\gamma$ -Al<sub>2</sub>O<sub>3</sub> and Pt/Rh/CeO<sub>2</sub>/ $\gamma$ -Al<sub>2</sub>O<sub>3</sub> in the Presence of H<sub>2</sub>O and CO<sub>2</sub>, *J. Catal.* 171 (1997) 358–373.
- [43] G. Nikolaidis, T. Baier, R. Zapf, G. Kolb, V. Hessel, W.F. Maier, Kinetic study of CO preferential oxidation over Pt–Rh/ $\gamma$ -Al<sub>2</sub>O<sub>3</sub> catalyst in a micro-structured recycle reactor, *Catal. Today* 145 (2009) 90–100.
- [44] V. Russo, T. Kilpiö, J. Hernandez Carucci, M. Di Serio, T.O. Salmi, Modeling of microreactors for ethylene epoxidation and total oxidation, *Chem. Eng. Sci.* 134 (2015) 563–571.
- [45] F. Ebrahimi, E. Kolehmainen, A. Laari, H. Haario, D. Semenov, I. Turunen, Determination of kinetics of percarboxylic acids synthesis in a microreactor by mathematical modeling, *Chem. Eng. Sci.* 71 (2012) 531–538.
- [46] H. Zhao, S. Liu, M. Shang, Y. Su, Direct oxidation of benzene to phenol in a microreactor: Process parameters and reaction kinetics study, *Chem. Eng. Sci.* 246 (2021) 116907.
- [47] G. Li, S. Liu, X. Dou, H. Wei, M. Shang, Z.H. Luo, Y. Su, Synthesis of adipic acid through oxidation of K/A oil and its kinetic study in a microreactor system, *AIChE J.* 66 (2020) e16289.
- [48] T.A. Nijhuis, J. Chen, S.M.A. Kriescher, J.C. Schouten, The direct epoxidation of propene in the explosive regime in a microreactor—a study into the reaction kinetics, *Ind. Eng. Chem. Res.* 49 (2010) 10479–10485.
- [49] Z. Vajgllová, N. Kumar, K. Eränen, M. Peurla, D.Y. Murzin, T. Salmi, Ethene oxychlorination over CuCl<sub>2</sub>/ $\gamma$ -Al<sub>2</sub>O<sub>3</sub> catalyst in micro- and millistructured reactors, *J. Catal.* 364 (2018) 334–344.
- [50] G. Wu, E. Cao, P. Ellis, A. Constantinou, S. Kuhn, A. Gavriilidis, Continuous flow aerobic oxidation of benzyl alcohol on Ru/Al<sub>2</sub>O<sub>3</sub> catalyst in a flat membrane microchannel reactor: An experimental and modelling study, *Chem. Eng. Sci.* 201 (2019) 386–396.
- [51] J. Singh, N. Kockmann, K.D.P. Nigam, Novel three-dimensional microfluidic device for process intensification, *Chem. Eng. Process. Process Intensif.* 86 (2014) 78–89.
- [52] Y. Maralla, S.H. Sonawane, Process intensification by using a helical capillary microreactor for a continuous flow synthesis of peroxypropionic acid and its kinetic study, *Periodica Polytechnica Chem. Eng.* 64 (2019) 9–19.
- [53] A. Tušek, A. Aalić, B. Zelić Kurtanek, Modeling and kinetic parameter estimation of alcohol dehydrogenase-catalyzed hexanol oxidation in a microreactor, *Eng. Life Sci.* 12 (2012) 49–56.
- [54] A.A. Mirzaei, A. Pourdolat, M. Arsalanfar, H. Atashi, A.R. Samimi, Kinetic study of CO hydrogenation on the MgO supported Fe–Co–Mn sol–gel catalyst, *J. Ind. Eng. Chem.* 19 (2013) 1144–1152.
- [55] N. Mahata, V. Vishwanathan, Kinetics of phenol hydrogenation over supported palladium catalyst, *J. Mol. Catal. A: Chem.* 120 (1997) 267–270.
- [56] N. Joshi, A. Lawal, Hydrodeoxygenation of 4-propylguaiacol (2-methoxy-4-propylphenol) in a microreactor: performance and kinetic studies, *Ind. Eng. Chem. Res.* 52 (2013) 4049–4058.
- [57] S. Vahid, A.A. Mirzaei, An investigation of the kinetics and mechanism of Fischer-Tropsch synthesis on Fe–Co–Ni supported catalyst, *J. Ind. Eng. Chem.* 20 (2014) 2166–2173.
- [58] A.A. Mirzaei, E. Reza zadeh, M. Arsalanfar, M. Abdouss, M. Fatemi, M. Sahebi, Study on the reaction mechanism and kinetics of CO hydrogenation on a fused Fe–Mn catalyst, *RSC Adv.* 5 (2015) 95287–95299.
- [59] A. Tanimu, S.A. Ganiyu, O. Muraza, K. Alhooshani, Palladium nanoparticles supported on ceria thin film for capillary microreactor application, *Chem. Eng. Res. Des.* 132 (2018) 479–491.
- [60] K. Maresz, A. Ciemięga, J. Mrowiec-Białoń, Monolithic microreactors of different structure as an effective tool for in flow MPV reaction, *Chem. Eng. J.* 379 (2020) 122281.
- [61] A.A. Mirzaei, M. Farahi, M. Akbari, Effect of reduction and reaction conditions on the catalytic performance of Co–Ni/Al<sub>2</sub>O<sub>3</sub> catalyst in CO hydrogenation: modeling of surface reaction rate, *Chem. Pap.* 75 (2021) 2087–2103.
- [62] V. Vishwanathan, V. Jayasri, P. Mahaboob Basha, Vapor phase hydrogenation of o-chloronitrobenzene (o-CNB) over alumina supported palladium catalyst – a kinetic study, *React. Kinet. Catal. Lett.* 91 (2007) 291–298.
- [63] F.E. Massoth, P. Politzer, M.C. Concha, J.S. Murray, J. Jakowski, J. Simons, Catalytic hydrodeoxygenation of methyl-substituted phenols: correlations of kinetic parameters with molecular properties, *J. Phys. Chem. B* 110 (2006) 14283–14291.

- [64] P.E. Savage, S. Gopalan, T.I. Mizan, C.J. Martino, E.E. Brock, Reactions at supercritical conditions: Applications and fundamentals, *AIChE J.* 41 (1995) 1723–1778.
- [65] E. Ramírez, F. Recasens, M. Fernández, M.A. Larrayoz, Sunflower oil hydrogenation on Pd/C in SC propane in a continuous recycle reactor, *AIChE J.* 50 (2004) 1545–1555.
- [66] E.V. Rebrov, A. Berenguer-Murcia, H.E. Skelton, B.F.G. Johnson, A.E.H. Wheatley, J.C. Schouten, Capillary microreactors wall-coated with mesoporous titania thin film catalyst supports, *Lab Chip* 9 (2009) 503–506.
- [67] S. Chatani, C.J. Kloxin, C.N. Bowman, The power of light in polymer science: photochemical processes to manipulate polymer formation, structure, and properties, *Polym. Chem.-UK* 5 (2014) 2187–2221.
- [68] Y. Su, V. Hessel, T. Noël, A compact photomicroreactor design for kinetic studies of gas-liquid photocatalytic transformations, *AIChE J.* 61 (2015) 2215–2227.
- [69] M.L. Satuf, J. Macagno, A. Manassero, G. Bernal, P.A. Kler, C.L.A. Berli, Simple method for the assessment of intrinsic kinetic constants in photocatalytic microreactors, *Appl. Catal. B* 241 (2019) 8–17.
- [70] G. Yu, N. Wang, Gas-liquid-solid interface enhanced photocatalytic reaction in a microfluidic reactor for water treatment, *Appl. Catal. A* 591 (2020) 117410.
- [71] X. Shi, S. Liu, C. Duanmu, M. Shang, M. Qiu, C. Shen, Y. Yang, Y. Su, Visible-light photooxidation of benzene to phenol in continuous-flow microreactors, *Chem. Eng. J.* 420 (2021) 129976.
- [72] D.D. Phan, F. Babick, T.H.T. Trnh, M.T. Nguyen, W. Samhaber, M. Stintz, Investigation of fixed-bed photocatalytic membrane reactors based on submerged ceramic membranes, *Chem. Eng. Sci.* 191 (2018) 332–342.
- [73] T. Aillet, K. Loubière, L. Prat, O. Dechy-Cabaret, Impact of the diffusion limitation in microphotoreactors, *AIChE J.* 61 (2015) 1284–1299.
- [74] N. El Achi, F. Gelat, N.P. Cheval, A. Mazzah, Y. Bakkour, M. Penhoat, L. Chausset-Boissarie, C. Rolando, Sensitized [2+2] intramolecular photocycloaddition of unsaturated enones using UV LEDs in a continuous flow reactor: kinetic and preparative aspects, *React. Chem. Eng.* 4 (2019) 828–837.
- [75] Y. Takahashi, A. Nagaki, Anionic polymerization using flow microreactors, *Molecules* 24 (2019) 1532.
- [76] C.O.C. López, Z. Fejes, B. Viskolcz, Microreactor assisted method for studying isocyanate-alcohol reaction kinetics, *J. Flow Chem.* 9 (2019) 199–204.
- [77] L. Qiu, K. Wang, S. Zhu, Y. Lu, G. Luo, Kinetics study of acrylic acid polymerization with a microreactor platform, *Chem. Eng. J.* 284 (2016) 233–239.
- [78] L. Xiang, Y. Song, M. Qiu, Y. Su, Synthesis of branched poly(butyl acrylate) using the strathclyde method in continuous-flow microreactors, *Ind. Eng. Chem. Res.* 58 (2019) 21312–21322.
- [79] P. Wang, K. Wang, J. Zhang, G. Luo, Preparation of poly(*p*-phenylene terephthalamide) in a microstructured chemical system, *RSC Adv.* 5 (2015) 64055–64064.
- [80] S.S. Cutie, P.B. Smith, D.E. Henton, T.L. Staples, C. Powell, Acrylic acid polymerization kinetics, *J. Polym. Sci. Pol. Phys.* 35 (1997) 2029–2047.
- [81] J. Huang, F. Sang, G. Luo, J. Xu, Continuous synthesis of Gabapentin with a microreaction system, *Chem. Eng. Sci.* 173 (2017) 507–513.
- [82] C. Du, J. Zhang, G. Luo, Organocatalyzed Beckmann rearrangement of cyclohexanone oxime in a microreactor: Kinetic model and product inhibition, *AIChE J.* 64 (2018) 571–577.
- [83] L. Li, J. Zhang, C. Du, K. Wang, G. Luo, Kinetics study of sulfuric acid alkylation of isobutane and butene using a microstructured chemical system, *Ind. Eng. Chem. Res.* 58 (2018) 1150–1158.
- [84] M. Shang, T. Noël, Y. Su, V. Hessel, Kinetic study of hydrogen peroxide decomposition at high temperatures and concentrations in two capillary microreactors, *AIChE J.* 63 (2017) 689–697.
- [85] J.S. Zhang, Y.C. Lu, Q.R. Jin, K. Wang, G.S. Luo, Determination of kinetic parameters of dehydrochlorination of dichloropropanol in a microreactor, *Chem. Eng. J.* 203 (2012) 142–147.
- [86] K. Shibatani, K. Fujii, Reaction of poly(vinyl alcohol) with formaldehyde and polymer stereoregularity - model compounds, *J. Polym. Sci. Part A-1-Polym. Chem.* 8 (1970) 1647.